

**EXTRACTION AND DEPROTEINATION OF
EXTRACTED SILK FIBERS FROM SILK
COCOON AND DEVELOPMENT OF
HYDROPHILIC ELECTROSPUN SILK FIBERS**

NURUL AFIQAH BINTI MOHD ZAKI

**FACULTY OF ENGINEERING
UNIVERSITY OF MALAYA
KUALA LUMPUR**

2016

**EXTRACTION AND DEPROTEINATION OF EXTRACTED SILK
FIBERS FROM SILK COCOON AND DEVELOPMENT OF
ELECTROSPUN SILK FIBERS**

NURUL AFIQAH BINTI MOHD ZAKI

**RESEARCH REPORT SUBMITTED IN PARTIAL FULFILMENT
OF THE REQUIREMENTS FOR THE DEGREE OF MASTER OF
ENGINEERING**

**FACULTY OF ENGINEERING
UNIVERSITY OF MALAYA
KUALA LUMPUR**

2016

UNIVERSITY OF MALAYA
ORIGINAL LITERARY WORK DECLARATION

Name of Candidate: Nurul Afiqah Binti Mohd Zaki

Matric No: KGL 140013

Name of Degree: Biomedical Engineering

Title of Project Paper/Research Report/Dissertation/Thesis: Extraction and Deproteination of Extracted Silk Fibers from silk cocoon and Development of Hydrophilic Electrospun Silk Fibers

Field of Study: Biomaterial

I do solemnly and sincerely declare that:

- (1) I am the sole author/writer of this Work;
- (2) This Work is original;
- (3) Any use of any work in which copyright exists was done by way of fair dealing and for permitted purposes and any excerpt or extract from, or reference to or reproduction of any copyright work has been disclosed expressly and sufficiently and the title of the Work and its authorship have been acknowledged in this Work;
- (4) I do not have any actual knowledge nor do I ought reasonably to know that the making of this work constitutes an infringement of any copyright work;
- (5) I hereby assign all and every rights in the copyright to this Work to the University of Malaya ("UM"), who henceforth shall be owner of the copyright in this Work and that any reproduction or use in any form or by any means whatsoever is prohibited without the written consent of UM having been first had and obtained;
- (6) I am fully aware that if in the course of making this Work I have infringed any copyright whether intentionally or otherwise, I may be subject to legal action or any other action as may be determined by UM.

Candidate's Signature

Date:

Subscribed and solemnly declared before,

Witness's Signature

Date:

Name:

Designation:

ABSTRACT

Silk fibroin protein derived from *Bombyx Mori* silk cocoon is a natural polymer that widely used for application in tissue engineering. Silk Fibroin has remarkable properties that demonstrates biocompatibility, biodegradable and great mechanical properties. In this present study, regenerated silk fibroin can be obtained by multistep preparation which are degumming and solubilisation process. The small pieces of regenerated silk fibers were cut and then blended with Polyvinylalcohol (PVA) solution to enhance the mechanical property of scaffold. Electrospinning capable to fabricate scaffold with the high surface area. Result showed that by increased of concentration of solution silk/PVA, voltage and flowrate, more fibers were produced in the film. A thin white film was produced at film of silk/PVA at 14% (w/v) without addition of chloroform. Scanning Electron Microscope (SEM) investigated the morphology of silk and revealed that applied voltage of 15kV during electrospinning has narrowest of fiber diameter (0.270 μm), less number of beaded, smaller beads and high average size of pore (1.379 μm). Flowrate parameter showed that more electrospun fibers were produced at 3 ml/h with fiber diameter (0.357 μm). The water contact angle measures the hydrophilicity of silk film where at 15 kV and 3 ml/h has highest in hydrophilicity with contact angle 27.3° and 20.1° respectively. The Fourier Transform Infrared (FTIR) spectroscopy was used to characterize the raw cocoon, degummed silk, regenerated silk fibroin and silk/PVA solution. FTIR spectra showed that new characteristic peak of Amide III at 1445 to 1458 cm^{-1} presence in degummed silk, regenerated silk fibroin and silk/PVA solution. The result indicate that β sheet was formed after degumming process. The result also indicated that all peaks at silk/PVA solution have become stronger with addition of PVA content due to chemical bonding of silk and PVA. The silk/PVA based scaffold produced by dialysis free technique in this study can be promising candidate as biomaterial for various tissue engineering application.

ABSTRAK

Protein fibroin sutera yang diperolehi daripada kepompong *Bombyx Mori* adalah polimer semula jadi yang digunakan secara meluas dalam aplikasi kejuruteraan tisu. Sutera fibroin mempunyai ciri-ciri luar biasa yang menunjukkan keserasian bio, biodegradasi dan tahap mekanikal yang bagus. Untuk kajian ini, sutera fibroin diperolehi dengan pelbagai langkah iaitu proses nyahgam dan proses solubiliti. Gentian sutera fibroin dipotong kecil-kecilan dan dicampur dengan larutan Polyvinylalcohol (PVA) untuk meningkatkan daya mekanikal dalam penghasilan perancah. Electrospinning berupaya untuk membentuk perancah dengan kawasan permukaan yang tinggi. Ia didapati bahawa peningkatan konsentrasi, voltan dan kadar aliran dapat menghasilkan lebih banyak serat dalam filem. Lapisan putih kelihatan pada filem silk/PVA pada 14% (w/v) tanpa penambahan chloroform. Scanning Electron Magnification (SEM) menyiasat morfologi sutera dan didapati pada 15kV mempunyai diameter fiber yang halus ($0.270\ \mu\text{m}$), jumlah manik yang sedikit, size yang kecil dan size liang yang tinggi ($1.379\ \mu\text{m}$). Pada kadar aliran menunjukkan yang gentian fiber lebih banyak terhasil pada 3 ml/h dengan diameter fiber ($0.357\ \mu\text{m}$). Water Contact Angle menguji tahap hidrofilik filem dimana pada 15 kV dan 3 ml/h mempunyai tahap hidrofilik paling tinggi dimana 27.3° and 20.1° . Fourier Transform Infrared (FTIR) digunakan untuk mencirikan kepompong, degummed sutera, penghasilan sutera fibroin dan larutan silk/PVA. FTIR spectra menunjukkan terdapat ciri baru iaitu Amide III pada 1445 ke $1458\ \text{cm}^{-1}$ di nyahgam sutera, penghasilan sutera fibroin dan larutan silk/PVA. Hasilnya menunjukkan bahawa pembentukan lembaran β dihasilkan selepas proses degumming. Hasil kajian juga menunjukkan bahawa semua kemuncak pada sutera/PVA telah menjadi lebih kuat dengan penambahan PVA melalui ikatan kimia oleh sutera dan PVA. Perancah silk/PVA dengan menggunakan teknik tanpa dialisis mampu dijadikan sebagai biomaterial untuk digunakan untuk pelbagai aplikasi kejuruteraan tisu.

ACKNOWLEDGEMENTS

Glory to be Allah S.W.T the Almighty, all the praise to His Prophet Muhammad S.A.W. I am very grateful to Allah S.W.T for His Blessing and Grace for giving me self-confidence and help in my endeavors and bringing me this far to complete this project. I would like to express my gratitude to my supervisor Associate Professor Ir. Dr. Belinda Murphy for her invaluable guidance throughout this research, comments and constructive criticisms greatly enhanced this project dissertation. I have been amazingly fortunate to have a supervisor who gave me the freedom to explore on my own and at the same time the guidance to recover when my steps faltered. Special thanks to Dr, Sumit Pramanik for his innovative ideas, support and enlighten discussion that drive me to explore the area of research in depth with the spirit of adventure. Apart from that, I would like to thank Nazira Bt Zubir for assist me in sourcing of cocoon. Besides, my friends for their support and help me to stay focused on my study. Finally, I want to thank my beloved father Mohd Zaki Bin Shaaban and family for their moral support, helpfulness, patience and outstanding throughout my study. My sincere appreciation also extends to everyone who has contributed to completion of this project study even indirect or direct. I hope that my research from this study would give benefit and extra knowledge to myself and to everyone.

TABLE OF CONTENTS

Abstract	iv
Abstrak	v
Acknowledgements	vi
Table of Contents	vii
List of Figures	ix
List of Tables.....	xi
List of Symbols and Abbreviations.....	xii
List of Appendices	xiii
CHAPTER 1: INTRODUCTION	1
1.1 Biomaterials in Biomedical Applications	1
1.2 Silk Fibroin as a Biomaterial	3
1.3 Electrospun Silk Fibers	5
1.4 Objectives.....	6
CHAPTER 2: LITERATURE REVIEW	7
2.1 Silk Fibroin Extraction.....	7
2.1.1 Comparison of Methods in Degumming	7
2.1.2 Comparison of Methods in Solubilisation.....	8
2.1.3 Comparison of Materials that used in Solubilisation.....	10
2.2 Electrospinning Technology	14
2.2.1 Electrospinning Principle.....	14
2.2.2 Electrospinning Constraint	15
2.3 Silk as Scaffold in Biomedical Application.....	16
CHAPTER 3: MATERIALS AND METHODOLOGY.....	18

3.1 Extraction of Silk Fibroin.....	18
3.2 Electrospinning Solution.....	21
3.3 Electrospinning Device	22
3.4 Characterization Methods	23
CHAPTER 4: RESULT & DISCUSSION	24
4.1 Visual Inspection.....	24
4.2 Fiber Morphology	26
4.2.1 Effect of Applied Voltage in Electrospinning	26
4.2.2 Effect of Flowrate in Electrospinning.....	31
4.3 Fiber Mat Wettability	38
4.4 Identification of Chemical Compound.....	40
CHAPTER 5: CHAPTER 5: CONCLUSION AND FUTURE STUDIES.....	42
REFERENCES	44
APPENDIX A	48
APPENDIX B	53
APPENDIX C	54

LIST OF FIGURES

Figure 2.1: SEM micrograph for silk fibroin fibers treated with LiBr (a) and CaCl ₂ (b) at 10000 x magnification. (Kamalha et al., 2014, pg.203&204).....	11
Figure 2.2: Schematic diagram of set up of electrospinning apparatus a) vertical set up, b) horizontal set up. From R. Anamariga (2014) Electrospinning process: Versatile preparation method for biodegradable and natural polymers and biocomposite systems applied in tissue engineering and drug delivery. Retrieved from https://www.researchgate.net/publication	15
Figure 2.3: Histological view of the groups at 4 weeks postoperatively. A-control group, B-SS group, C-PDLSS group & D-DPSS groups at 40 magnification, Mason's trichrome staining. (Park et al., 2015, pg.5)	17
Figure 3.1: Degummed silk after treated with Na ₂ CO ₃ solution before (a) and after (b) drying for 24 hours.....	19
Figure 3.2: The dried silk fibers after treated with CaCl ₂ after drying for 24 hours	19
Figure 3.3: The schematic diagram of silk fibroin extraction process.....	20
Figure 3.4: The mixture of small cut fibers with PVA solution.....	21
Figure 3.5: Electrospinning horizontal setup	22
Figure 3.6: Water Contact Angle instrumentation	23
Figure 3.7: Fourier Transform Infrared Spectroscopy (FTIR).....	23
Figure 4.1: The film of concentration of silk/PVA solution(14% w/v) and chloroform (a) 28%(w/v), (b) 32%(w/v) and (c) 0%(w/v).....	24
Figure 4.2: The morphology of fiber at different voltage (a) 10kV, (b) 15 kV and (c) 20 kV with 15000x magnification.....	27
Figure 4.3: Fiber diameter of electrospun fiber at 10kV.....	27
Figure 4.4: Fiber diameter of electrospun fiber at 15kV.....	28
Figure 4.5: Fiber diameter of electrospun fiber at 20kV.....	28
Figure 4.6: The histogram of diameter of electrospun fibers at 10kV, 15 kV and 20 kV	29
Figure 4.7: The histogram of pore size distribution at 10 kV, 15 kV and 20 kV.....	31

Figure 4.8: The morphology of fiber at different flowrate (a) 2ml/h, (b) 2.5 ml/h and (c) 3 ml/h with 15000x magnification.	32
Figure 4.9: Fiber diameter of electrospun fiber at 2ml/h	32
Figure 4.10: Fiber diameter of electrospun fiber at 2.5 ml/h	33
Figure 4.11: Fiber diameter of electrospun fiber at 3ml/h	33
Figure 4.12: The histogram of diameter of electrospun fibers at 2, 2.5 and 3 ml/h.....	34
Figure 4.13: The histogram of pore size distribution at 2, 2.5 and 3 ml/h.....	36
Figure 4.14: Contact angle of electrospun silk/PVA fiber mat with different voltage and flowrate	38
Figure 4.15: Water droplet on electrospun Silk/PVA.....	39
Figure 4.16: The FTIR spectrum of cocoon, degummed silk, regenerated silk and silk/PVA based scaffold.....	41

LIST OF TABLES

Table 2.1: Degummed silk extracted by various method in degumming process.	7
Table 2.2: The benefits and limitations of solvent in silk treatment.	13
Table 4.1: The average, minimum and maximum diameter of 10 kV, 15 kV and 20 kV	29
Table 4.2: The average size of pore and total pore distribution of each voltage	31
Table 4.3: The average, minimum and maximum diameter of 2, 2.5 and 3 ml/h.....	34
Table 4.4: The average size of pore and total pore distribution of each flowrate.....	35

University of Malaya

LIST OF SYMBOLS AND ABBREVIATIONS

CA	:	Contact Angle
ECM	:	Extracellular Matrix
FDA	:	Food and Drug Administration
FTIR	:	Fourier Transform Infrared
MSC	:	Mesenchymal Stem Cell
PVA	:	Polyvinylalcohol
SEM	:	Scanning Electron Microscope
SF	:	Silk Fibroin
TFF	:	Tangential Flow Filtration

University of Malaya

LIST OF APPENDICES

Appendix A: Image J Software (Fiber Diameter)	48
Appendix B: Image J Software (Pore Size)	53
Appendix C: FTIR Spectra	54

University of Malaya

CHAPTER 1: INTRODUCTION

1.1 Biomaterials in Biomedical Applications

Biomaterial can be defined as a biological or synthetic substance that can be inserted into body tissue to interact with biological system as part of a medical implant, device, coating substance or replace an organ with similar functionality. The main usages of biomaterial in biomedical applications are joint replacement, artificial ligament and tendons, dental implant, suture and skin repair devices (Donaruma, 1988). The main criterion as biomaterials is they must be biocompatible with human body, where the ability of material to perform with an appropriate host response (Ulery, Nair & Laurecin, 2012).

Materials that have been used in biomedical applications are composed from metals/alloys, ceramics, and glasses to polymers. Polymers have great potential since they have high mechanical strength, hydrolytically degradable, can be fabricated into a tailored architecture and has approval of Food and Drug Administration (FDA) (Gunatillake & Adhikari, 2003). The most commonly used synthetic polymers are poly (glycolic acid) (PGA), polyurethanes, poly (vinyl acid) (PVA) and poly (lactic acid) (PLA). These synthetic polymers have widely been used in cardiovascular applications, skin artificial and bone tissue engineering in biomedical applications. Despite various advantageous of these synthetic polymers, they often showed lack of biocompatibility, bioactivity and biodegradability which are necessary criteria for biomedical applications (Caló & Khutoryanskiy, 2015).

Researchers have shifted from synthetic polymers into natural polymers to counter the disadvantageous of synthetic polymers to have better biocompatibility, biodegradability, and bioactivity. The common natural biomaterials that have been used so far are protein-based such as fibroin and collagen, while polysaccharides-based are hyaluronic acid,

alginate, chitosan, and so on. These can be found in extracellular matrix component (ECM) that composed naturally and typically promote excellent cell proliferations (Hinderer, et al., 2016). In this context, silk fibers had shown better biocompatibility with substantial mechanical properties (Zhao et al., 2005).

Recently, there are a lot of studies on bio composite of silk since the silk alone is lack in mechanical strength and thermal properties and not suitable for tissue engineering. These properties can be boosted by blending silk fibroin with natural polymer such as collagen, chitosan, Hydroxyapatite or with synthetic polymer such as Polyethylene oxide, Polyvinyl alcohol, Polylactic acid and other biocompatible material (Bowlin et al., 2010). One of the study, silk fibroin/chitosan based scaffold have been fabricated and the cross linking between these two material were found able to improve the properties such as tensile strength, surface hardness and thermal stability (Thenmozhi, Gomathi & Sudha, 2013). Silk/hydroxyapatite composite scaffold were investigated for bone tissue regeneration. The content of hydroxyapatite able to enhance the osteogenic property as well as increasing the stiffness of scaffold that suitable for bone regeneration (Huang et al., 2015). Silk blending with polyethylene oxide (PEO) showed that properties of surface at silk film were improved as compare to pure silk film. Furthermore, the silk/PEO scaffold generate scaffold with unique morphology and definable porosity (Jin et al., 2004).

1.2 Silk Fibroin as a Biomaterial

Silks are natural fibrous protein polymers that can be extracted from a variety of insect's larvae to form cocoon. Spiders also produce silk fibers but the amount produced is less than silkworm cocoon. They form silk for their protection, support, capturing food and reproduction (Guinea, et al., 2015). Silk from *Bombyx Mori* had been used widely in textile industries for decades. Nowadays, silk fibroin has gained popularity as biomaterial due to their remarkable properties such as highly strength, lightweight, biocompatibility, biodegradable and no or negligible immune response by the host. Properties of silk is well known for strong natural fiber, hydrophobic and thermal stability and good resistance to deformation. The properties of silk is highly depending on the sources and environment (Das et al., 2014). The applications of silk as biomaterial already have been approved by FDA for suture over several decades (Cao & Wang, 2009). Silk had been widely explored in the field of tissue engineering and regenerative medicine. Silk scaffolds had been used in various types of connective tissues such as bone, cartilage tendon and ligament (Thilagavathi & Viju, 2015).

The *Bombyx Mori*, also known as silkworm, is normally found with have cocoon shell that is typically in oval shape with a range 4 cm in length and commonly in white color. It is able to tolerate in topical environment and generally found in topical country such as Malaysia, Indonesia, Thailand and China (Nualkaew, Wongsanta & Damrongrungrueng, 2012). The cocoon from *Bombyx Mori* is a unique material. It contains of two types of protein such as sericin and fibroin. Sericin is an outer layer that covers the periphery of the raw silk fibers. Sericin acts as an adhesive which maintains the structure of cocoon. The physical properties of sericin are highly soluble in aqueous solution and can easily be removed in degumming process (Addis & Raina, 2013). This is because that sericin is

highly hydrophilic protein that is composed of amino acid groups such as serine (25%), aspartic acid (17%), threonine (6%) and glutamic acid (5%) (Gimenes et al., 2014).

On the other hand, silk fibroin is the inner layer that consists of layers of antiparallel β sheets. Silk fibroin has higher potential in biomedical applications than the sericin due to its physical properties derived from its backbone structure. The structure of silk fibroin is consisted of block copolymers that are rich in beta-sheet that linked with hydrogen bonding (Marelli et al., 2016). The β crystalline structure mainly contributes to its high mechanical strength. Within these crystalline domains there are some subdomains that are rich in glycine (46%), alanine (30%), and serine (12%) (Rockwood et al., 2011). In term of degradation, highly crystallized silk degrades in vivo slowly that commonly spends over 60 days to degrade as compare with lower in silk crystallinity that usually take 7-15 days. However, the degradation of scaffold in vivo is depend on the implantation site (Teuschl et al., 2015).

1.3 Electrospun Silk Fibers

Electrospinning is a very efficient technique for fabrication of nanofibrous scaffolds for tissue engineering. Fabrication of scaffold can be generate into 2D and 3D constructs, for examples such as flat sheets or cylindrical sheets (Pramanik et al., 2012). Various formats of electrospun silk fibroin (SF) had been further processed into films, hydrogels, sponges, nets and meshes after degumming and solubilisation process (Huemmerich et al., 2006). In addition, parameters such as type of substrates, solutions and processing can be manipulate to obtain the desired properties of scaffold. These surface modification of silk fibroin scaffold can affect the response of cell toward material.

Electrospun scaffold can mimic the topographies of extracellular matrix (ECM) that should display remarkable physical features such as substantial porosity and pore sizes to allow cell interaction via diffusion of oxygen and nutrient. Other important criteria of scaffold are recognition and elicit response to the target cells. Numerous studies shown about cell adhesion, proliferation and regeneration of tissue in vitro as well in vivo condition of electrospun scaffold in tissue engineering (Zhang et al., 2010). Typically, randomly distributed fibers are collected during electrospinning and forming woven or non-woven fibrous mats (Meinel et al., 2013). The characteristic of non-woven mat are the rough surface topography, high porosity and pore distribution and large fiber diameter. In contrast, the woven mats of silk fibroin are fabricated closely mimic the native structure by hierarchical arrangement of fibers. The woven mats usually favorable in cellular growth by high attachment due to its similarity with nature tissue. The regeneration of a range of tissues such as osteoblast, vascular tissue, epithelial tissue, fibroblast, connective tissue had been studied (Koh et al., 2015).

1.4 Objectives

The objectives of the study are :-

1. To study the process of silk fibroin extraction with dialysis free method.
2. To fabricate composite scaffold from silk fibroin fiber blended with PVA solution by implementing electrospinning technique.
3. To characterize the scaffold morphologies by manipulation of parameters in electrospinning.
4. To analyze the scaffold characteristic using Water Contact Angle, SEM, and FTIR method.

University of Malaya

CHAPTER 2: LITERATURE REVIEW

2.1 Silk Fibroin Extraction

Silk fibroin extraction is a multistep preparation that include degumming and solubilisation process. Degumming is a process separation of sericin and fibroin and removal of sericin. Next step, the extracted silk fibroin can be obtained through solubilisation process. The end result is an aqueous solution of pure silk fibroin that can be further used for production of scaffold.

2.1.1 Comparison of Methods in Degumming

Silk is comprised of fibroin that can be found in the inner layer and sericin at the outer layer of cocoon. Notably that fibroin is mostly used in biomedical application due to non-immunogenic response compare with sericin. Silk Fibroin can be extracted by degumming process that can be performed in many method such as classical, physical, enzyme and acid as shown in Table 2.2.

Table 2.1: Degummed silk extracted by various method in degumming process. (Vyas & Shukla, 2016)

Method	Characteristic	Result
Classical	Treatment with 'Marseille soap', then be removed by boiling off and washed with weakly ammonia.	Gentlest way of degumming but expensive. Neutralized soap solution has no degumming action on silk.
Physical	Treatment with water under pressure at 121°C / Treatment with ultrasound at -180°C,	Sericin is not removed completely.
Enzymatic	Treatment with enzyme such as papain or trypsin, removed by using boiled hot water and followed by weakly alkaline solution (sodium bicarbonate) or acidic solution (tartaric, citric acid).	Complete degumming cannot be done with enzymatic action. Enzyme is used as alternative to reduce pollution level and ability to preserve the physical properties of silk.
Acid	Treatment with tartaric acid or dichloro, trichloro acetic acid for 30 minutes.	The sericin have been removed completely at higher concentration but also increasing in weight loss.

2.1.2 Comparison of Methods in Solubilisation

After degummed process, silk fibroin must undergo solubilisation process where the solubilisation agent is used to convert from solid into liquid fibers. The solubilisation have been patented as far as mid 1930's (Pat. No. : US1966756) by Fritz Gajewski in July 1934. He used liquid ammonia as solvent to the degummed silk for dissolving fibroin. The fibroin were dissolved in liquid anhydrous ammonia of -77°C for 30 minutes. The solution become concentrated as evaporation of ammonia occurred during stirring of solution. As a result, honey colored aqueous solution is obtained by filtered the impurities using a nickel gauze. However this method is not favorable due to the usage of ammonia that is harmful to be implemented into human body (Fritz Gajewski, 1934).

Apart from using ammonia, salt can be used as alternative for dissolving silk fibroin. Salts can be removed through dialysis process to regenerated silk fibroin solution. Dialysis process means ions from solubilisation agent are removed from silk fibroin through the use of dialysis membrane and a series of water changes. There are a lots of studies that using dialysis in extraction of fibroin due to their promising result in the pure silk fibroin extraction. The common procedure for this process is the silk fibroin is dissolved in 9 M LiBr solution and this solution was dialyzed in water using cellulose membrane for several days. The dialysis process can preserve the chemical composition of silk because the gentle osmosis occur during the process. Harsh method will cause further destruction to the structural and chemical composition which further reduce the stability of silk. The mixture was further centrifuged to remove impurities and this yield high purification of silk fibroin solution (Cai et al.,2017; Ri et al.,; Singh, Panda & Pramanik, 2016). The limitations of this dialysis methods are this process is relatively slow for complete removal of salt and limited for scale up. In addition the usage of LiBr

is expensive compare to other solvent. After dialysis, the concentration of fibroin solution is usually too dilute to spin fiber threads (Cheung et al., 2008).

Due to limitations in dialysis process, many researchers have tested and developed alternatives to overcome the limitations with different methodologies for silk fibroin extraction. Invention that have been patented in 2012 by Jen et al. from Taipei indicated that regenerated silk fibroin can be done without dialysis step. This method applying a shear stress by using homogenizer to the silk fibroin dissolve in CaCl_2 solution to induced a phase separation in a period of time and changing solvent power of the fibroin solution. The solvent power is changed by lowering the proportion of salt in the solution. After precipitation, the silk fibroin can be further washed with deionized water to remove salt. The regenerated silk fibroin obtained from the process in organosoluble. This invention simplifies the process and shorten the process time from 1 to 2 hours whereas the conventional dialysis process would normally takes 1 to 3 days. This invention also claimed that it can increase productivity of silk fibroin at least 8% and have appropriate mass production (Jen et al., 2012).

Newest technology also involve free dialysis where it provides solubilisation using diafiltration technique. This technique has been patent by Bressner and Tilburey in 2016. Tangential flow filtration (TFF) is one of the technique that applies diafiltration to eliminate solubilisation agent. The process requires solution of silk fibroin and solubilisation agent passing through the system, the retentate contained a purified regenerated silk fibroin solution. The bed height and column diameter are proportional to the volume of solubilized silk fibroin to be purified. Alternatively, desalting column also can be used to separate solubilisation agent and silk fibroin. In addition, combining these two equipment where the product eluted from desalting column in concentrated and further purified using the TFF device. The benefit of these combination to allow for the

creation of silk solutions possessing tunable mechanical properties. This invention claimed that the regenerated silk fibroin can be directly converted into solid and gel products (Bressner & Tilburey, 2016).

2.1.3 Comparison of Materials that used in Solubilisation

The characteristic of fibroin protein is not soluble in water and roughly 76% of its amino acid have non-polar side chains. The insolubility of silk fibroin causes it to have difficulty dissolving in common solvents due to its high molecular weight and crystallinity. In addition, the presence of sericin and other impurities might also prevent the penetration of the solvent and result in lower solubility of silk fibroin (Addis & Raina, 2013). Regardless of these difficulties, the solubility of silk fibroin in certain solvents has been studied and several solvents have been successfully discovered for solubilisation. It has been known that salts can be dialyzed to produce fibroin solutions. Fibroin is soluble in high ionic aqueous salt solutions such as Lithium Thiocyanate (LiSCN), Sodium Thiocyanate (NaSCN), Zinc Chloride ($ZnCl_2$), Magnesium Chloride ($MgCl_2$) and copper salts such as Copper Nitrate ($Cu(NO_3)_2$), Copper Ethylene Diamine ($Cu(NH_2CH_2CH_2NH_2)_2(OH)_2$). However, many studies suggested using LiBr or $CaCl_2$ as solvents compared to copper salts because copper residues tend to remain in silk fibroin after dialysis. (He, Gui & Cui, 2011)

The strong alkali such as Lithium Bromide (LiBr) has a significant effect on the characteristics of silk. The treatment by using an aqueous LiBr solution produced liquid silk fibroin with a transparent dialyzed solution. An aqueous LiBr solvent is able to change the molecular structure of degummed silk by active ionic movement from lithium entering the crystal domain in fibroin fibers (Daithankar et al., 2005). Researchers from the Department of Textile Engineering, Donghua University have conducted an experiment regarding the

effects of LiBr and CaCl₂ concentration on morphology of electrospun Bombyx Mori silk. The SEM result in Figure 2.1 showed that nanofibers produced by LiBr as solvent slightly exhibit finer diameter and better distribution compare to solvent by CaCl₂. The silk film also been found that at lower concentration, the fibers are scattered and more discontinuously but produced thinner film with higher concentration (Kamalha et al, 2014). However, silk fibroin extraction using LiBr is very time consuming where it usually takes at least 48 hours in conventional dialysis to get the pure aqueous silk fibroin while the silk decompose by CaCl₂ is a little bit faster by takes only 24 hours.

Yang, Kwak and Lee in 2013 have conducted a study to investigate the effect of residual lithium ion on the silk fibroin film by using cytotoxicity test. They found that even after 72 hours of dialysis, the residual lithium ion is not completely removed. Even though the remained ions has acute toxicity but SF has low biodegradability therefore it will remained in the implantation site with a long period to fully degrade and prolonged exposure can bring harmful to the surrounding cells.(Yang, Kwak & Lee, 2013).

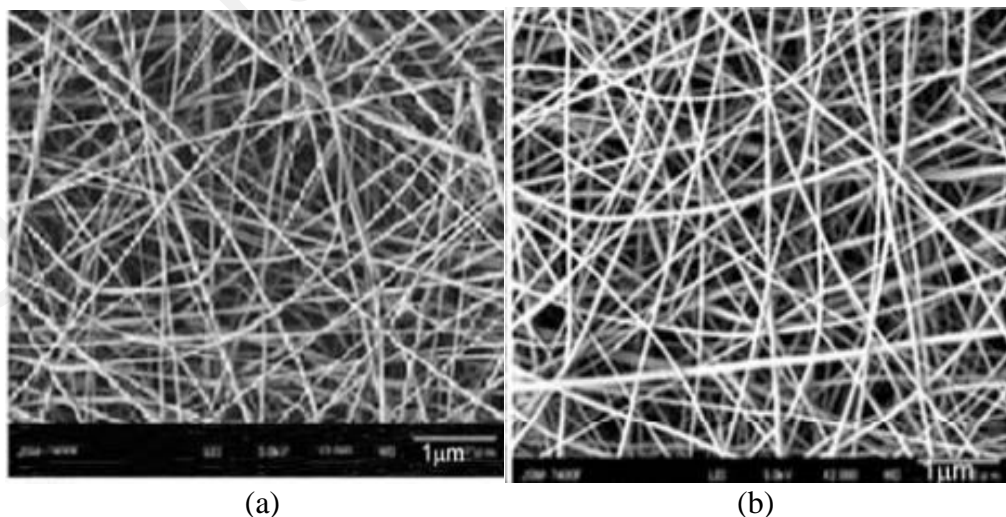


Figure 2.1: SEM micrograph for silk fibroin fibers treated with LiBr (a) and CaCl₂ (b) at 10000 x magnification. (Kamalha et al., 2014, pg.203&204)

On other hand, CaCl_2 have been intensively used as a solvent because it is cheaper compare to LiBr . A study had been conducted and reported that the solubility of Bombyx Mori silk fibroin increased sharply with higher concentration of CaCl_2 with addition of ethanol compare with CaCl_2 with addition water (Miyaguchi & Hu, 2005). Another study from H. Zhang et al., 2012 on treated of degummed Bombyx Mori with CaCl_2 and $\text{Ca}(\text{NO}_3)_2$ solution to analyzed the structure of these treated silk. Based on the result, CaCl_2 produced more crystalline structure by sharp peak compare to $\text{Ca}(\text{NO}_3)_2$ in X-Ray diffraction analysis. The advantage of this crystallinity is the more crystalline domain potential to decrease the degradation rate. The result also showed that the functional group of regenerated silk that treated with CaCl_2 were nearly similar to degummed silk compare to regenerated silk treated with $\text{Ca}(\text{NO}_3)_2$ (Zhang et al., 2012).

Apart from that, the chemical structure of regenerated silk fibroin prepared by lithium thiocyanate aqueous solution was investigated by Goto, Tsukada and Minoura in 1990 with different temperature at concentration of 9M were observed and have been found that optimum silk fibroin is at 40 °C which have 100 percent solubility. Composition of amino acid of regenerated silk fibroin is remained unchanged regardless of difference temperature. The result then compared with LiBr solution from other references and they found that silk fibroin were easily dissolved in LiSCN aqueous solution compared than in LiBr solution. However the morphology of silk fiber in LiSCN were not evenly distribution and large beaded as compared with LiBr aqueous solution (Goto, Tsukada & Minoura, 1990). Table 2.1 below showed the benefit and limitation of each solvent that have been used.

Table 2.2: The benefits and limitations of solvent in silk treatment.

Materials	Benefits	Limitations	References
LiBr	Higher solubility in silk fibroin, finer diameter and better distribution compare than CaCl ₂ solvent.	Expensive and time consuming in dialysis process.	(Daithankar et al., 2005) , (Kamalha et al, 2014)
CaCl ₂	Cheap, fibers produced more crystalline structure.	The fibers is less uniformity and fiber diameter is slightly large.	(H. Zhang et al., 2012)
Copper salt	Cheap and available.	Copper salt residue tend to remained in silk fibroin after dialysis process.	(He et al., 2011)
Lithium thiocyanate	Silk fibroin were easily dissolved.	Silk fibers are not evenly distribution and large beaded.	(Goto, Tsukada, Minoura ., 1990)

2.2 Electrospinning Technology

Nanofiber is generally a broad phase referring to fibrous structure with diameter less than 1 micron (Subramanian, Krishnan & Sethuraman , 2009). Nowadays, tissue engineering applications lend toward nanotechnology specifically nanofibers as artificial matrices due to its similarity to native extracellular matrix (ECM) (Zhang, Reagan & Kaplan, 2010). The electrospun nanofibers have higher surface areas, high interconnectivity and superior mechanical properties make it easy for functionalization for various purpose.

The fabrication technique is simple yet it can produced scale of sheet hence, electrospinning is favorable for many applications (Agarwal,Wenderoff & Greiner., 2008). In addition, variety morphology of scaffold can be produced by adjust parameters such as flow rate, voltage, rotation, needle size and solution concentration (Udaseen et al., 2014). Thus desired geometries and properties of scaffold can be produced if the appropriate parameters were chosen.

2.2.1 Electrospinning Principle

Electrospinning used two combination which are electrospray and spinning. A typical electrospinning setup consist of three components which are a high voltage, a needle and metal collector. Figure 2.2 show the schematic diagram of electrospinning that can be setup in vertical or horizontal. The high electric field which positive charge is applied to the metal needle. The negative charge is applied to the target or also called as collector is where the fibers are collected. As the attractive forces between metal needle and collector is increased, the more droplet away from the capillary and formed fibers at the surface of target. The polymer is solidifies as the solvent are evaporate to the air (Vonch, Yarin & Megaridis, 2007, X. Zhang et al., 2010, Meinel et al., 2013, Karakas, 2014).

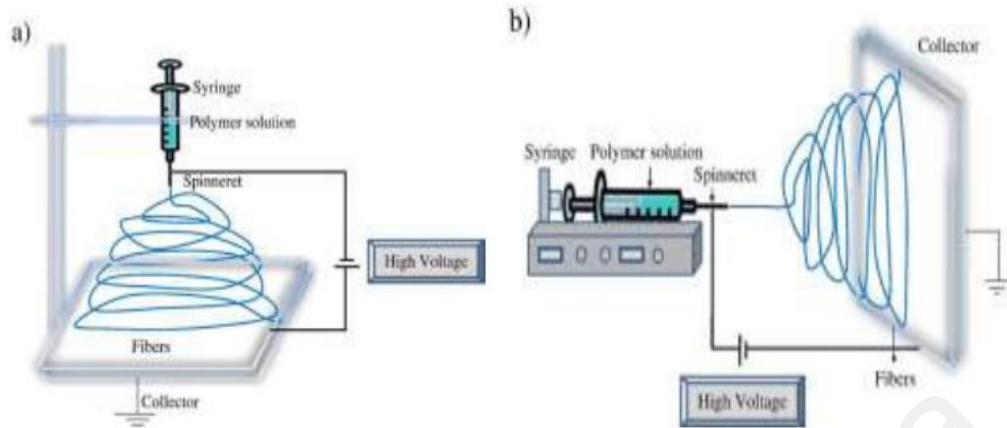


Figure 2.2: Schematic diagram of set up of electrospinning apparatus a) vertical set up, b) horizontal set up. From R. Anamariga (2014) Electrospinning process: Versatile preparation method for biodegradable and natural polymers and biocomposite systems applied in tissue engineering and drug delivery. Retrieved from <https://www.researchgate.net/publication>

2.2.2 Electrospinning Constraint

There are limitations with electrospinning such as uncontrollable scaffold morphology of the scaffold such as fiber diameter, randomness of alignment and sizes of beads. The formation of beads without defect still remain as a challenge in electrospinning. The outcome of scaffold is unpredictable due to highly depending on the processing parameter during electrospinning such as viscosity, concentration, chemical interaction and molecular weight of solution itself. This technique is only applicable to some type of polymers (Zhang et al., 2010, Wei & Kim, 2013).

Polymer usually dissolved in water or organic solvent such as formic acid, hexafluoroisopropanol (HFIP) or chloroform depending on the type of polymers. The solvent has a crucial role, it is needed to make sure the solution is viscous enough for polymer chain entanglement to occur thus fiber diameter will increased linearly. However, most of organic the solvent are highly toxic and if it is left in the scaffold can cause cell death (Sell et al., 2010). The danger of high voltage must be taken as precaution during handling the electrospinning where serious injuries can happen especially if electrical leakage is occur.

2.3 Silk as Scaffold in Biomedical Application

Silk scaffolds have been used in various types of connective tissues for examples ligament, tendon, cartilage and bone. Scaffold serves as a support that mimic the ECM to allow cells to migrate, proliferate and differentiate into tissues. Thus, the scaffold should consider biocompatibility feature, porosity with high surface area for exchange of gases, nutrient and waste, recognition of cell and elicit response (Wenk, Meinel, Wildy, Merkle, & Meinel, 2009).

In bone tissue engineering, the potential use of silk scaffold was investigated. A study was conducted to determine the osteogenic effect of human dental pulp and periodontal ligament derived cell in rabbits. The cells were seeded onto a 3D nano hydroxyapatite coated silk fibroin scaffold and implanted into rabbits. and the result showed that negligible amount of bone tissue formation was noticed where cells proliferate into the defect spaces after 4 weeks. Based on Figure 2.3, there are no significance changes in (A) where it is a control sample which no scaffold is added but the cell occupied the defect space in (B) silk scaffold (SS), (C) dental pulp cell seeded on SS (DPSS), periodontal ligament cell seeded on SS (PDLSS). Nano hydroxyapatite has capability to stimulate the cells for regeneration of new bone. The biocompatibility nHA-silk scaffold as osteoconductive as well as low immunogenicity and biodegradable have showed remarkable properties as biomaterial in tissue engineering especially in bone tissue engineering (Park et al., 2015).

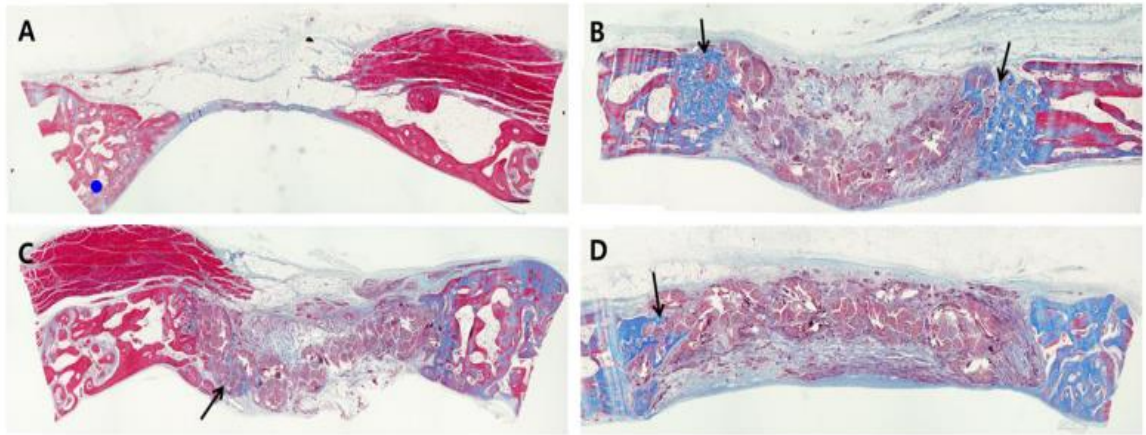


Figure 2.3: Histological view of the groups at 4 weeks postoperatively. A-control group, B-SS group, C-PDLSS group & D-DPSS groups at 40 magnification, Mason's trichrome staining. (Park et al., 2015, pg.5)

Adult mesenchymal stem cells (MSCs) have exhibited the potential to divide and differentiate into bone, cartilage, and fat cells in electrospun nanofibrous silk scaffold (Wang et al., 2005). A study by Navone et al., on in vitro cartilage tissue engineering using MSCs has successful repair of severe cartilage damage. The analysis were performed by scanning electron microscopy, Fourier Transform Infrared Spectroscopy and differential scanning calorimetry and the resulting MSC were adhere, grow on silk scaffold and able to maintain their phenotypic mesenchymal profile after 4 weeks of cultivation and able to mimic those in native articular cartilage tissue (Navone et al., 2014).

CHAPTER 3: MATERIALS AND METHODOLOGY

3.1 Extraction of Silk Fibroin

Bombyx Mori silkworm cocoon were purchased from Bogor, Western Java, Indonesia. First step was the separation of pupa from the cocoon followed by cleaning the cocoon with 70% alcohol. The dried cocoon was cut into small pieces. Next was the degumming process where the cocoon was boiled into stirred aqueous solution of sodium carbonate (Na_2CO_3) at 100°C for 40 minutes. The preparation of sodium carbonate (Na_2CO_3) solution was prepared by adding 0.3 gram of Na_2CO_3 powder into 150 ml of distilled water. Degummed fibers were recovered and washed with distilled water to remove the sericin protein that coat the silk fibroin protein as shown in Figure 3.1 (a). These silk fibers were squeezed and dried for 24 hours in an oven at 37°C in Figure 3.1 (b). 46% of degummed silk composition was water. After the drying process, the fiber was dissolved in aqueous CaCl_2 solution with 200 ml of 70% alcohol at 120°C for four hours. The CaCl_2 solution was prepared by adding 4.6 gram calcium oxide into 37% Hydrochloric acid (HCl) and 30 ml of distilled water. The fibers were washed again with distilled water for at least 12 times to remove the residue of solution remained in fibers before proceeded with drying process for 24 hours. The dried silk fibers obtained after treatment shown in Figure 3.2. The schematic diagram of silk extraction are shown in Figure 3.3.



(a) (b)
Figure 3.1: Degummed silk after treated with Na_2CO_3 solution before (a) and after (b) drying for 24 hours



Figure 3.2: The dried silk fibers after treated with CaCl_2 and dried for 24 hours

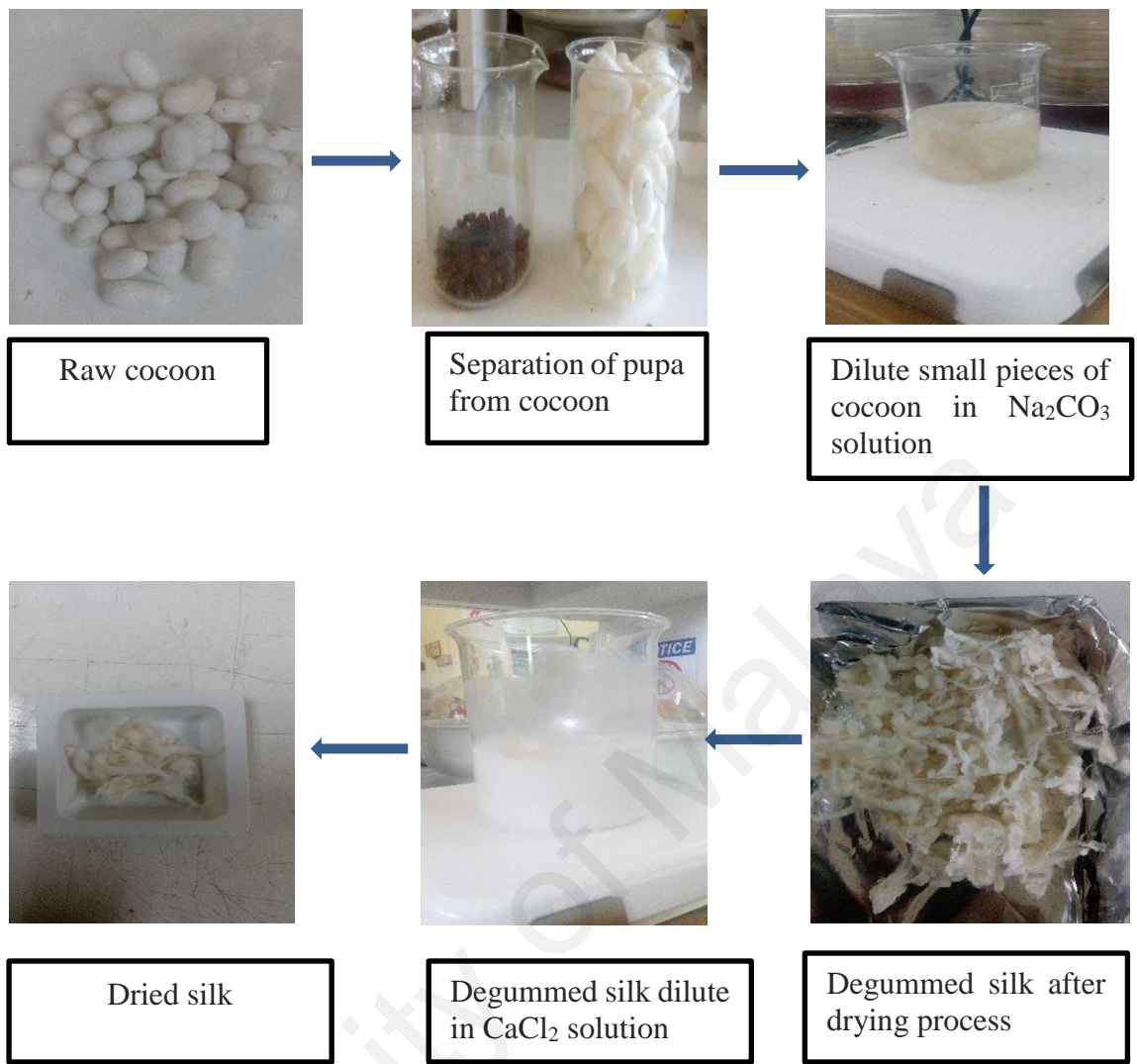


Figure 3.3: The schematic diagram of silk fibroin extraction process

3.2 Electrospinning Solution

The Polyvinylalcohol (PVA) solution was prepared by adding 1.8 g of PVA powder into 30 ml of water. The mechanical method is used where regenerated silk fibers were cut into small pieces of 0.3 g and added into PVA solution as shown in Figure 3.4. The solution was stirred for 24 hours and heated at 50°C before loaded to the 25 ml syringe.



Figure 3.4: The mixture of small cut fibers with PVA solution

3.3 Electrospinning Device

The electrospinning setup consist of high voltage direct current power supply, a needle, a syringe pump and grounded collector. The blue clip of crocodile wire that represents negative terminal is attached on the aluminium foil and another red clip represents positive terminal is attached at the needle. The applied voltage was in the range of 10-20 kV. The microscope slides (8cmx8cm) as center of target is attached on the aluminium foil. The syringe pump dispense the silk/PVA solution into needle that will form droplet at tip of needle as shown in Figure 3.5. The parameter such as feedrate, diameter of syringe pump and distance from needle to the aluminium foil were setup before running the electrospinning device. The films of silk /PVA fiber were collected from the microscope slide.

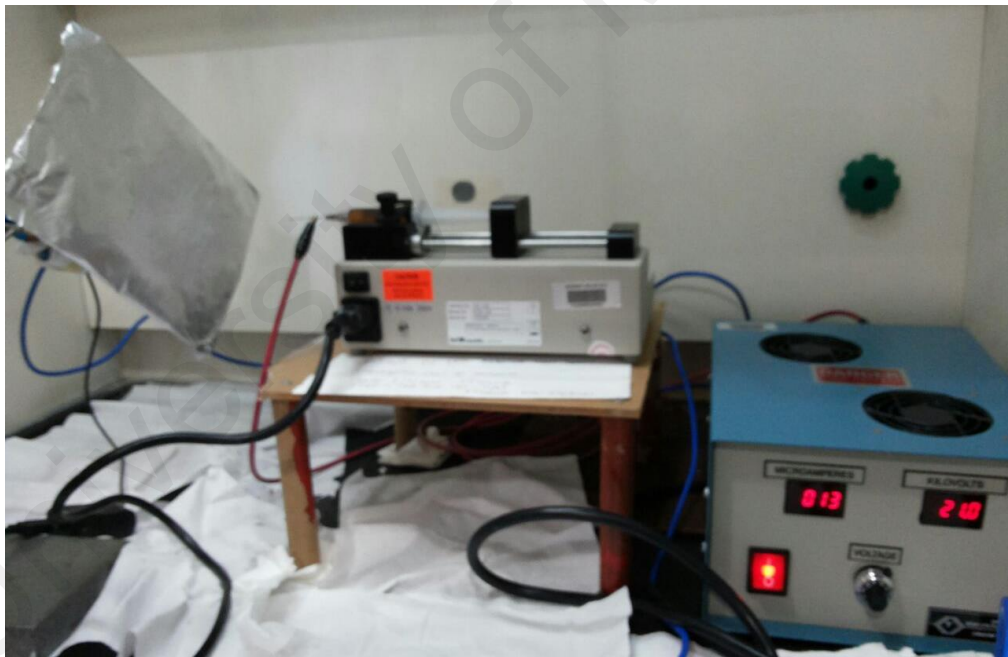


Figure 3.5: Electrospinning horizontal setup

3.4 Characterization Methods

The morphology of silk fiber was examined by Scanning Electron Microscope. Water contact analyzer was used to test materials hydrophilicity (Figure 3.6). The SCA20 software was used to construct the water contact angle on the film. The film was placed on the bottom of needle that contained distilled water. Dispense unit consist of dosing volume which is $2\mu\text{L}$ and dosing rate is $1.00\ \mu\text{L/s}$. The type of syringe used is B.Braun 1 ml disposable syringe. On the other hand, Fourier Transform infrared spectroscopy (FTIR) (ATR-FTIR400,Perkin Elmer) in the range of $4000\text{-}400\ \text{cm}^{-1}$ was used to analyze the functional group and chemical composition of 4 samples which are cocoon, degummed silk, regenerated silk and silk/PVA solution.

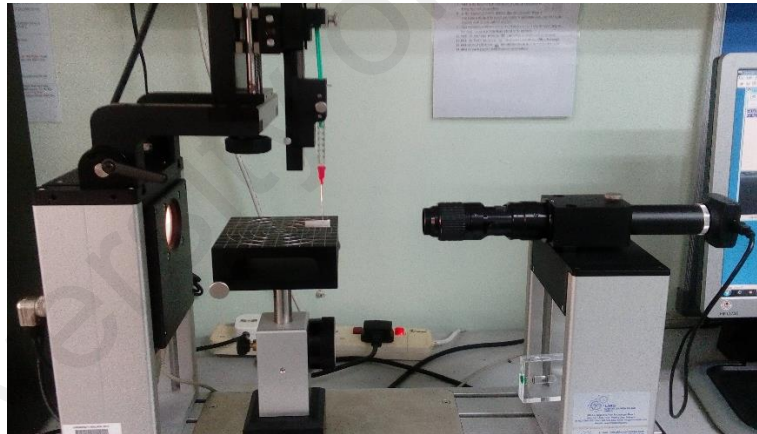


Figure 3.6: Water contact Angle instrumentation

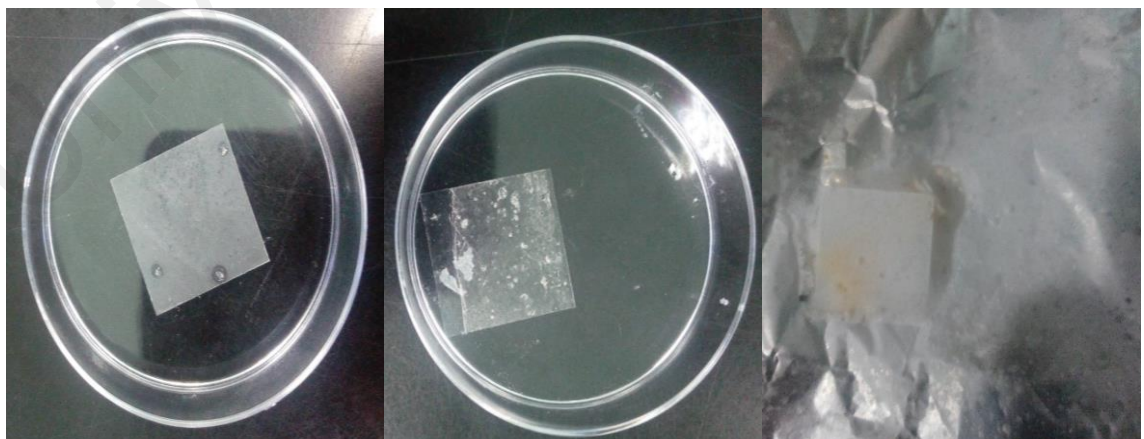


Figure 3.7: Fourier Transform Infrared Spectroscopy (FTIR)

CHAPTER 4: RESULT & DISCUSSION

4.1 Visual Inspection

The visual inspection was performed after electrospinning to determine the production of fibers on the target sample. The visual inspection consist of formation of white film on the surface on microscope cover slip that act as target. Two parameters affect the fibers formation during electrospinning process, namely solution parameter and processing parameter. The solution parameter is the concentration of silk/PVA solution. Three sheets of silk/PVA film of approximately size 10cmx10cm were produced as shown in Figure 4.1. Three types of solution were prepared with varies concentration such as silk/PVA solution concentration set at 14 % w/v and 28 % w/v of chloroform solvent, silk/PVA solution concentration set at 14 % w/v and 32 % w/v of chloroform solvent and lastly silk/PVA solution set at 14 % w/v without addition of chloroform. The concentration of silk/PVA solution has totally change by addition of chloroform where the concentration of solution become lower with present of chloroform meanwhile without addition of chloroform solvent make concentration of solution become higher.



(a) (b) (c)
Figure 4.1: The film of concentration of silk/PVA solution(14% w/v) and chloroform (a) 28%(w/v), (b) 32%(w/v) and (c) 0%(w/v)

Based on results, a thin white film was produced by silk/PVA solution without added chloroform solvent at Figure 4.1 (c). After 18 hours of electrospinning, the solution in (a) and (b) that were added with chloroform produced an inconsistency of film. The solution without added chloroform solvent gave more fibers with higher uniformity is due to concentration affect. The experiment also has been tested by using acetic acid as solvent with same amount of concentration however the result was worst compare with chloroform solvent which no thin white formation at all three type of solution. Thus the experiment was abandoned and proceed with chloroform solvent. The relationship of concentration of solution and fibers were the lower the concentration of solution, less fibers were obtained and vice versa. This is proved by Huan et al that, the combination of solvent has an effect on fibers morphology. When the concentration is so low, the polymeric nano particles obtained were in beads form rather that in fiber form. In contrast, as the concentration increased, a mixture of fibers and bead were obtained. However, lower concentration produced irregular beads due to insufficient in elongation of liquid jet hence droplets were formed (Huan et al., 2015). The reason of lack of drawing fibers in silk/PVA solution by addition of solvent were there are complete evaporation of solvent or uneven evaporation occurred from the thread by the time it's landed at the target. (Lee et al., 2003) Thus the silk/PVA solution without addition of chloroform have passed the visual inspection since white film was produced.

4.2 Fiber Morphology

4.2.1 Effect of Applied Voltage in Electrospinning

The range of voltage can affect the dynamic of liquid flow, dripping rate and especially the structural morphology of electrospun fibers. Although some researchers claimed that the effect of voltage was less significance on the diameter of fiber (Jacobs, Anandjiwala & Maaza, 2010). However, other groups have found that the higher voltage can facilitated larger diameter fiber. For example, Meinel et al. have reported that electrospun fibers become larger and uniform in high voltage compare to lower voltage. The reason of this is the high voltage have influence in stretching and accelerate the jet and avoid it to become droplet at the end of nozzle (Meinel et al., 2013).

In this present study, it was observed that different structural morphologies were obtained by different range of voltage as shown in Figure 4.2. Three different voltage of 10kV, 15kV and 20kV were individually applied for electrospinning 14% (w/v) silk/PVA solutions with flowrate setting at 2.5 ml/h and collection distance at 10 cm for 18 hours. The electrospun fibers at 10kV, Fig. 4.2 (a) showed inconsistency of fibers with lots of beaded. At 15 kV, Fig 4.2 (b) there are deficiency of fibers formation with less number of beaded and smaller in size. Meanwhile, electrospun fibers at 20 kV, Fig 4.2 (c) shown uniformity of fibers and size is quite narrow. Based on the numbers of fibers, electrospun fibers produced at 20 kV is greater than others. This possibility of this result is due to the increasing of applied voltage influenced the charged jet travelled to the target much faster hence collected more fibers.

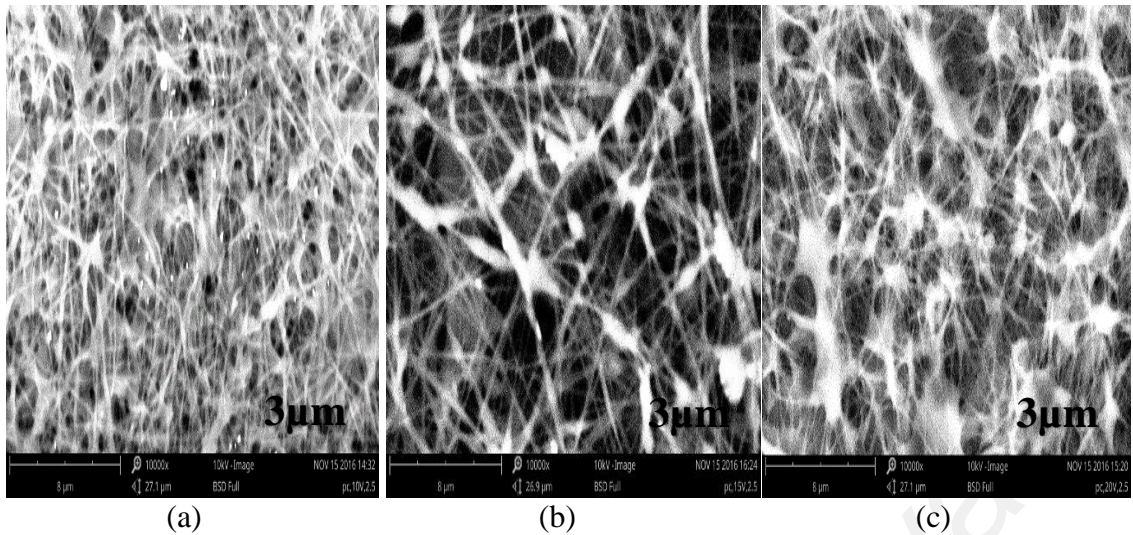


Figure 4.2: The morphology of fiber at different voltage (a) 10kV, (b) 15 kV and (c) 20 kV with 15000x magnification.

Fiber diameter can be measure based on SEM images using Image J software and can be referred to Appendix A. In this software, 20 randomly picked of fibers was selected for calculation of fibers diameter as shown in Figure 4.3 to Figure 4.5. From these graph, the pattern of fibers diameter as well as frequency, average, minimum and maximum value of 20 randomly picked of fibers can be easily determined. The pattern of fibers at 10 kV have fewer randomness in fibers diameter compared to 15 kV and 20 kV diameter fibers.

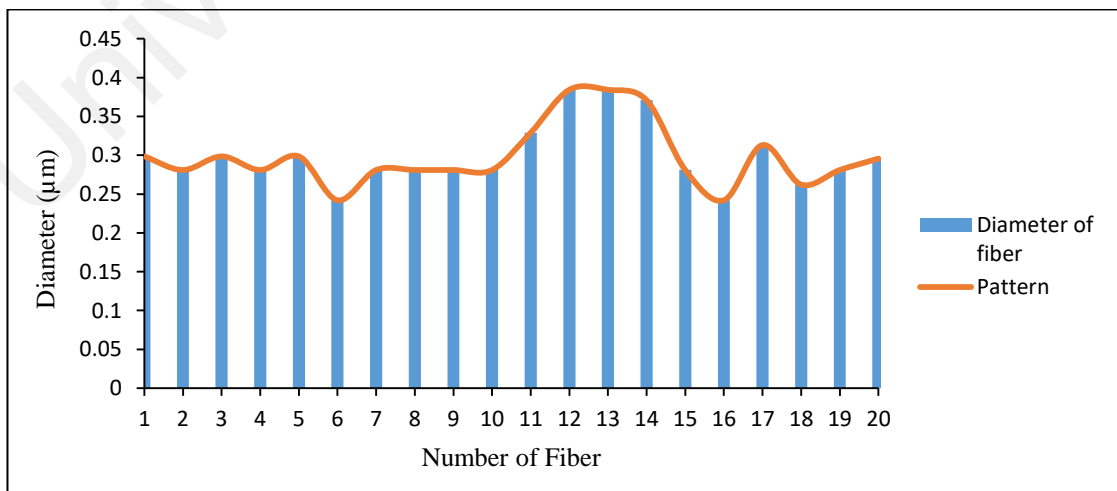


Figure 4.3: Fiber diameter of electrospun fiber at 10kV

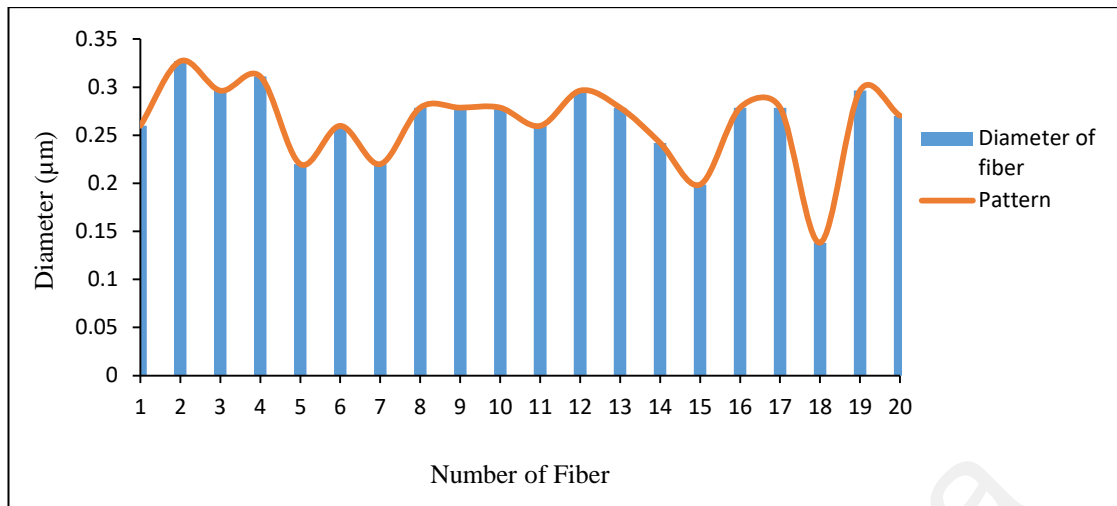


Figure 4.4: Fiber diameter of electrospun fiber at 15kV

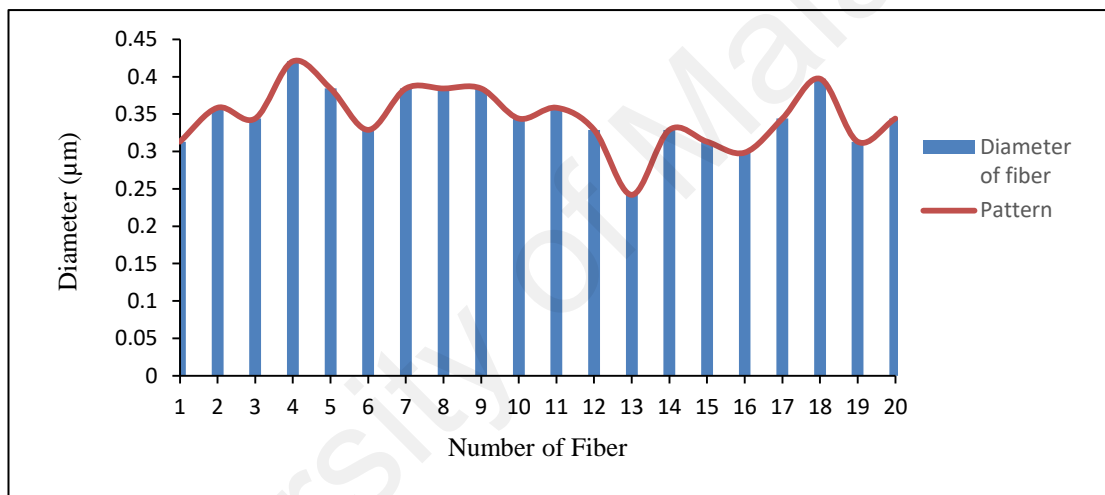


Figure 4.5: Fiber diameter of electrospun fiber at 20kV

Table 4.1 displays an average fiber diameter of $0.296 \pm \mu\text{m}$ at 10 kV, while the voltage of 15 kV and 20 kV yielded average diameters of $0.270 \pm \mu\text{m}$ and $0.346 \pm \mu\text{m}$ respectively. From these results, it was shown that the distribution of fiber diameter was broad at the 10 kV, narrow at 15 kV and broad again at 20 kV. This can be explained by relationship between three major factors which are Coloumbic forces, viscoelastic and surface tension in formation of fiber diameter. At low applied voltage, the Coloumbic forces is not high thus the attraction from droplet at tip of syringe to the target is decreased then resulting in less fiber with large diameter. At the moderate applied voltage, all three factors were well balanced because the narrow distribution of fiber diameter. With higher applied

voltage, the Coloumbic force is greater and produced more fibers with larger diameter. However, when the voltage is too high, it also resulted bead defect due to less time for liquid evaporation (Huan et al., 2015). The histogram of the diameter for 10kV, 15 kV and 20 kV are shown in Figure 4.6.

Table 4.1: The average, minimum and maximum diameter of 10 kV, 15 kV and 20 kV

Voltage (kV)	Average diameter of 20 randomly fibers(μm)	Minimum(μm)	Maximum(μm)
10	0.296 \pm	0.242	0.384
15	0.270 \pm	0.138	0.407
20	0.346 \pm	0.242	0.421

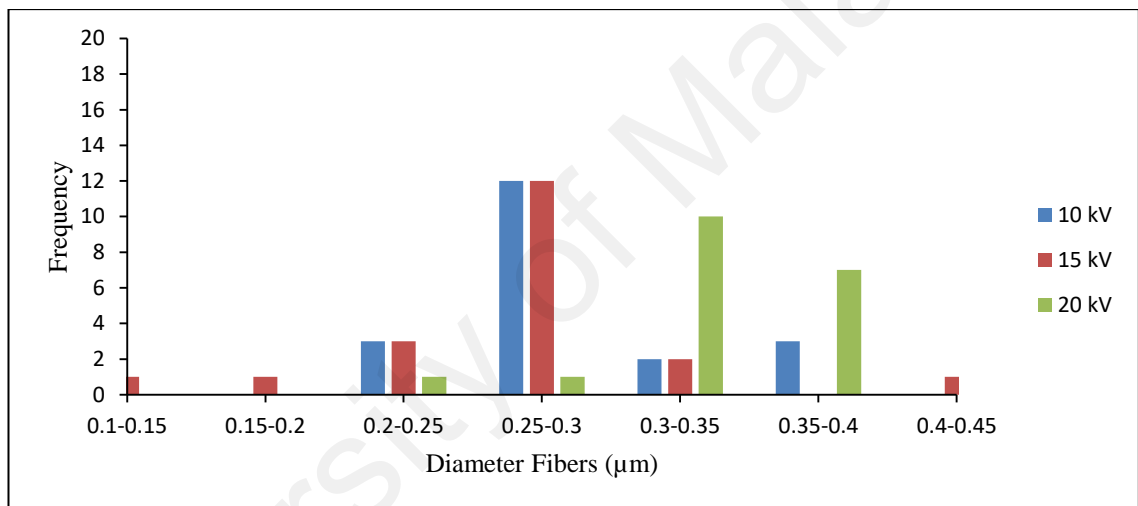


Figure 4.6: The histogram of diameter of electrospun fibers at 10kV, 15 kV and 20 kV

The effect of scaffold pore size and interconnectivity always have been related with the degradation rate of scaffold either in vivo or in vitro for most tissue engineering applications. For tissue engineering scaffold, one of main criteria is that the degradation rate should match the rate of new tissue regeneration. Based on Figure 4.7, the highest pores size distribution is same for 10 kV and 15 kV which is between 0.05 μm to 0.09 μm . For 20 kV, the highest value for pore size distribution is between 0.1 μm to 0.49 μm . In table 4.2, shows the average size of pore and total number of pore distribution for each voltage. The average size of pore have been calculated by using image J software (refer to Appendix B). Average size of pore at 15 kV is highest which is $1.379\pm \mu\text{m}$ and 20 kV is lowest which is $0.377\pm \mu\text{m}$. The total pore distribution at 10 kV is highest compare to others thus can be concluded that scaffold produce at 10 kV has highest porosity.

Study from Luo et al., demonstrate the degradation rate of silk fibroin scaffold based on pore size, pore density and size of internal pore wall. The result obtained showed that the highest porosity exhibit a faster rate of weight loss during degradation as compare with small porosity number that the scaffold is remained intact and the rate of degradation is relatively slow (Luo et al., 2015). In summary, the fibers produced at film applied voltage of 15 kV were less than 10kV and 20kV. However, it has less number of beads, small size of beads and smallest fiber diameter (0.138 μm). The average size of pore at 15 kV is the highest size ($1.379\pm \mu\text{m}$) with medium total distribution of pore.

Table 4.2: The average size of pore and total pore distribution of each voltage

Voltage	10kV	15kV	20kV
Average size of pore (μm)	$1.091\pm$	$1.379\pm$	$0.377\pm$
Total pore distribution	6226	3622	247

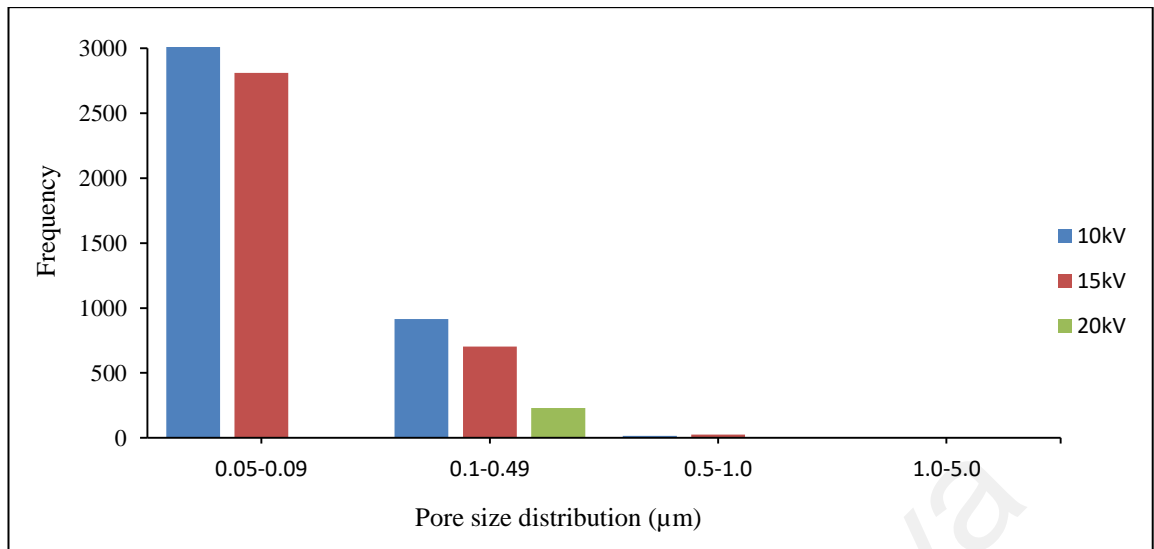


Figure 4.7: The histogram of pore size distribution at 10 kV, 15 kV and 20 kV

4.2.2 Effect of Flowrate in Electrospinning

Flow rate is also consider as one of the factor that control the fiber diameter and its distribution, maintenance of Taylor cone and deposition area (Zargham et al., 2012). Flow rate also can increase the fiber diameter but also led to bead defect such as braches and spitting. Silk/PVA blend solution were prepared at 14% (w/v) and been carried out with the same collective distance (10 cm) and same voltage applied (15kV) at the room temperature in the fume hood. The flow rate varied from 2.0, 2.5 and 3.0 ml/h. In this present study, Figure 4.8 shows the effect of flowrate on the morphology of electrospun fibers. It can be seen from SEM images (Figure 4.8) that cluster of beads were formed and the randomness of fibers at 2 ml/h. At 2.5 ml/h, there are larger beads and lack of fibers formation but less number of beaded. At 3ml/h, it look like there is well balance between more fibrous formation and average number of beaded with small size of beaded.

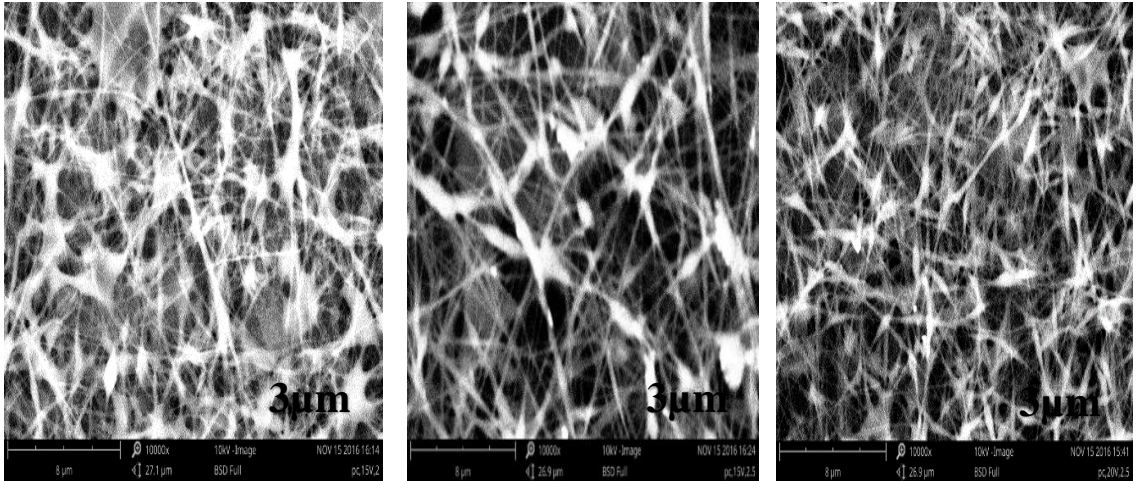


Figure 4.8: The morphology of fiber at different flowrate (a) 2ml/h, (b) 2.5 ml/h and (c) 3 ml/h with 15000x magnification.

The fiber diameter and number of pore distribution were measured using Image J software. Electrospun fibers can be produced with a range diameter by typically 0.1-100 μm. (Eichhorn & Sampson, 2010) In this software, 20 randomly picked fibers were selected for calculation of fibers diameter as shown in Figure 4.9 to Figure 4.11. Pattern of fiber diameter for 2 ml/h is not consistent. For 3 ml/h, the fibers diameter at first have randomly value but have not fluctuate as much as other two flow rates.

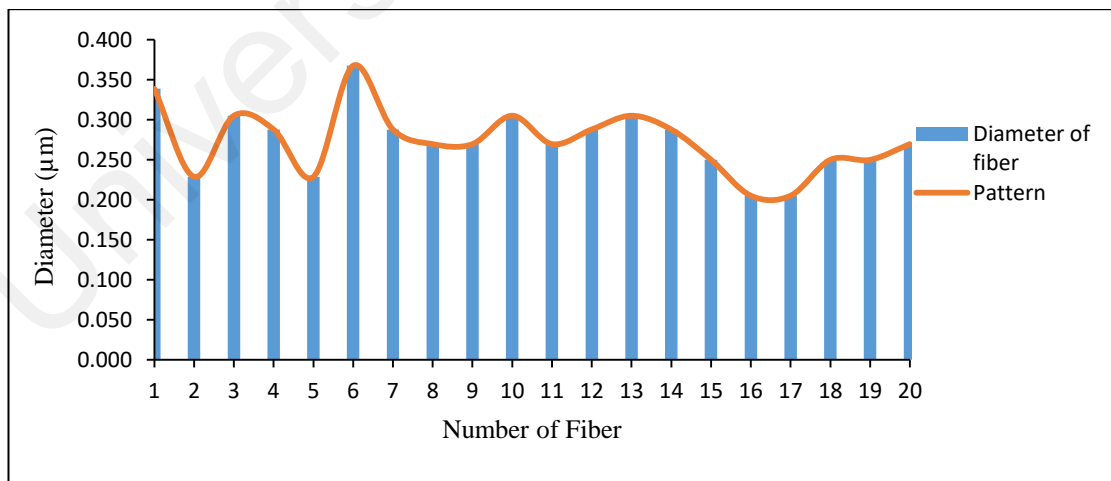


Figure 4.9: Fiber diameter of electrospun fiber at 2ml/h

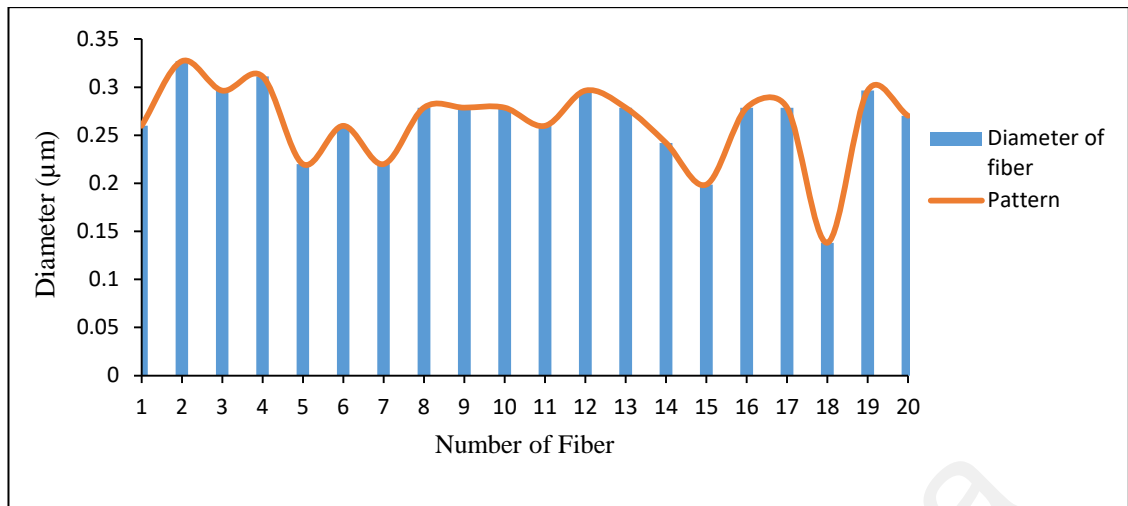


Figure 4.10: Fiber diameter of electrospun fiber at 2.5 ml/h

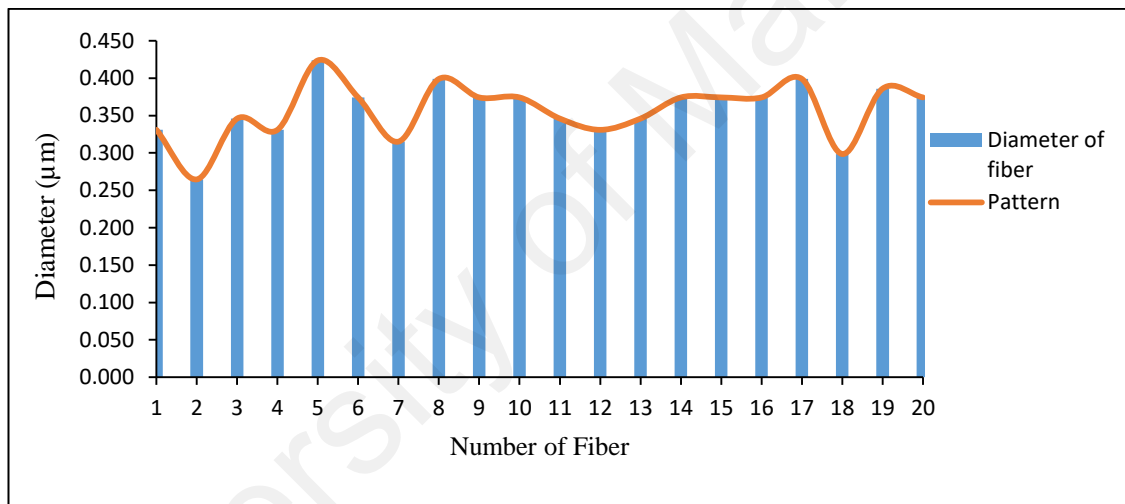


Figure 4.41: Fiber diameter of electrospun fiber at 3ml/h

Table 4.3 displays the average fiber diameter at 2 ml/h is $0.273 \pm \mu\text{m}$, while at 2.5ml/h and 3 ml/h yielded average diameter of $0.270 \pm \mu\text{m}$ and $0.357 \pm \mu\text{m}$ respectively. It shows that fiber diameter was about the same at 2ml/h and 2.5ml/h but wider at 3ml/h. It can be seen that diameter of electrospun fibers increased with higher flow rate. (Tang, Xu & Liu, 2014) has reported similar observation through theoretical analysis. The experimental result showed that with the increased of flow rate, the diameter of electrospun increases and diameter can be tunable by controlling the flow rate in electrospinning process.

Zargham et al., reported that morphologies of the electrospun nylon 6 nanofibers at 10 kV were effected by flow rate. At lower flowrate will caused the dripped of solution at capillary tip. This was due to influence of electrical charge that unable to draw a great volume of droplets. Very high flow rate resulting in high amount of solution being electro sprayed with thick diameter of beaded rather than smooth and thin fiber. (Zargham et al., 2012). Generally, at suitable flow rate, considerable amount of solution ejected from the capillary tips to the target contribute to fibers uniformity and enough time for solution for dry. In term of morphology, the narrowest fiber diameter and continuous fibers can be achieved. Figure 4.12 showed that most of fibers out 20 randomly picked fibers were produced in the range of diameter 0.25 to 0.3 μm at 2ml/h and 2.5 ml/h, while at 3ml/h is 0.35 to 0.4 μm .

Table 4.3: The average, minimum and maximum diameter of 2, 2.5 and 3 ml/h

Flowrate (ml/h)	Average diameter of 20 randomly fibers (μm)	Minimum(μm)	Maximum(μm)
2	0.273 \pm	0.205	0.367
2.5	0.27 \pm	0.138	0.407
3	0.357 \pm	0.265	0.424

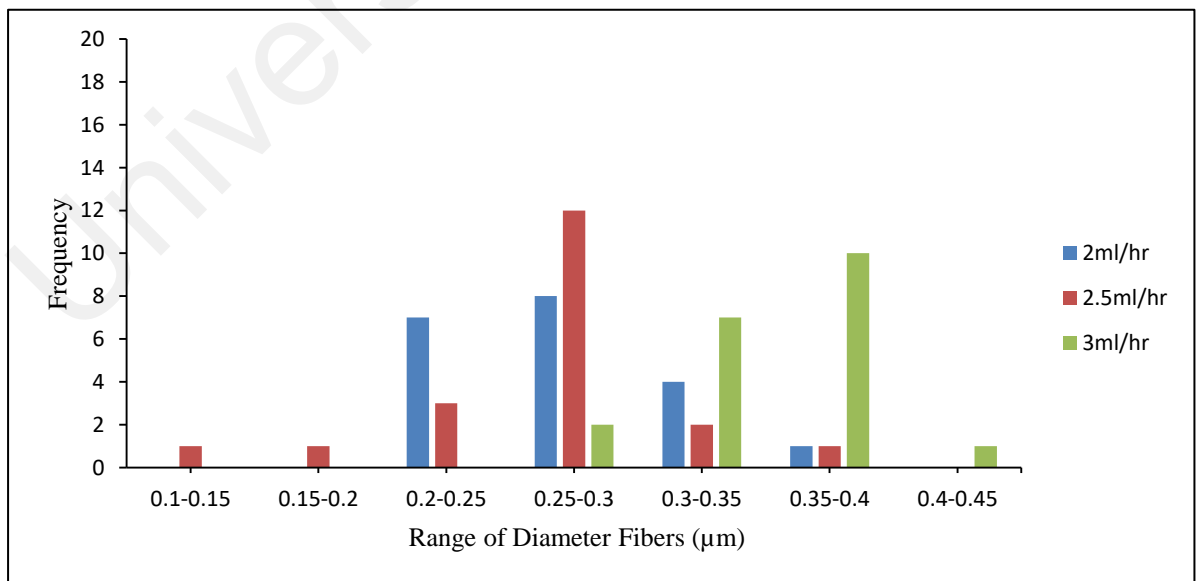


Figure 4.52: The histogram of diameter of electrospun fibers at 2, 2.5 and 3 ml/h

The adhesion and proliferation of cell on electrospun scaffold are affected by porosity, pore interconnectivity and large surface area. The average pore size and total number of pore distribution for different flow rate is displayed at Table 4.4. The highest pore size is measured 2.5 ml/h with 1.379 μm and the smallest value is at 2 ml/h with 0.547 μm . Pores size that too small is not favorable since it does not promote adequate growth of cell and minimize the migration of cell. While for pore size that too large, the surface area is decrease hence limiting the cell attachment and proliferation (Agarwal, Wenderoff & Greiner., 2008).

Rnjak-Kovacina and Weiss et al., have suggested that conversion of conventional electrospinning to wet electrospinning has increase the pore size of poly (glycolic acid) and silk fibroin for bone tissue engineering application. The pore size of electrospun silk fibroin has increase from 1.3-2.4 μm to 586-931 μm in wet electrospinning process. Another technique is salt leaching where porogen is used to increased pore size (Rnjak-Kovacina & Weiss, 2011). In summary, the fibers produced at flowrate 3 ml/h exhibit narrowest fibers diameter (0.270 μm) with average number of beaded and small size of beaded as compared to 2 ml/h and 2.5 ml/h.

Table 4.4: The average size of pore and total pore distribution of each flowrate

Flowrate	2ml/h	2.5ml/h	3ml/h
average size of pore (μm)	0.547 \pm	1.379 \pm	0.692 \pm
Total pore distribution	1410	3622	3307

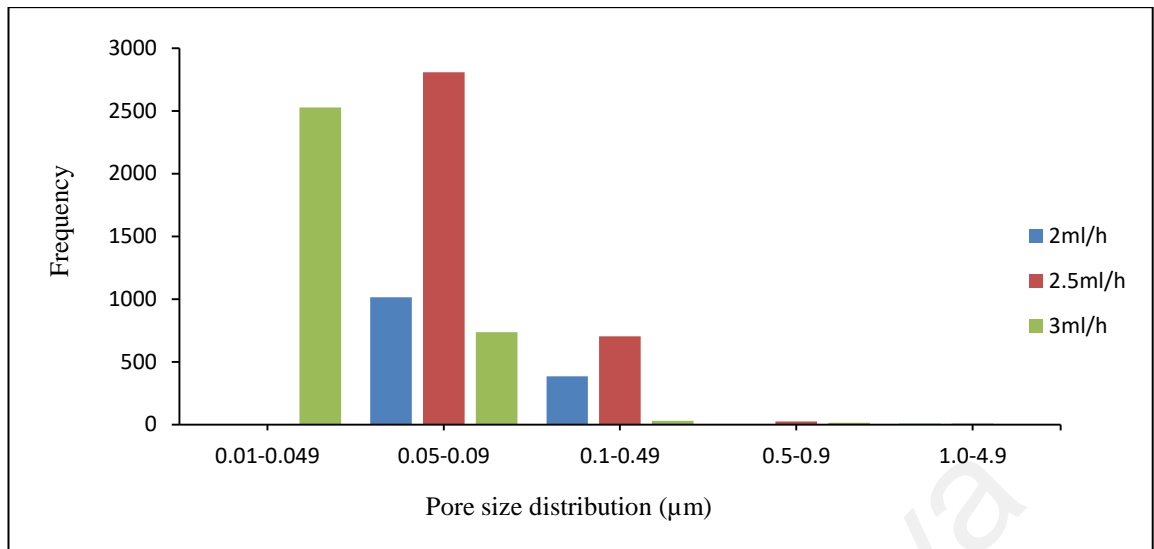


Figure 4.63: The histogram of pore size distribution at 2, 2.5 and 3 ml/h

Based on morphologies at all results in voltage and flowrate, the morphologies of silk/PVA scaffold in this project does not follow the criteria of ideal scaffold. The ideal scaffold in tissue engineering need to have uniform fibers without beaded, high interconnectivity and appropriate number of porous. There are a few factors that silk/PVA scaffold in this study does not achieved the ideal scaffold criteria. Firstly is the silk/PVA solution without usage of solvent in electrospinning where most of studies has use solvent in electrospinning in production of silk scaffold. The solution for this problem is to find suitable solvent for silk/PVA solution such as that able elongate the uniformity of fibers without beads such as ethanol, HFIP or methanol. The other factor is that the silk and PVA is not homogenously mixed in solution during electrospinning. The regenerated silk fibroin obtained through extraction is in solid form by using free dialysis technique. The difference between extraction with dialysis method and extraction dialysis free method were the form of silk fibroin. The silk fibroin obtained through dialysis is in liquid form thus it can be easily homogenized with other solvent. Meanwhile the silk fibroin obtained by not doing dialysis method is that the silk fibroin is in solid state. Although the solid silk fibroin have difficulty to homogenously mix with PVA but have similar chemical compound with liquid silk fibroin based on FTIR analysis. The solution

for this problem is shake the mixture of silk/PVA solution properly before electrospinning. The parameters such as distance, size of needle, molecular weight, surface tension and surface charge density also need to consider in order to produce desired scaffold.

University of Malaya

4.3 Fiber mat wettability

The surface structure of the electrospun mat plays a leading role in determining the hydrophobicity or hydrophilic properties. The roughness of the electrospun mat was affected by beads, porous and large fibers. The large fiber diameter and beads cause the surface of roughness to increase and led to hydrophobicity of surface. This is because the roughness of surface can trap more air which improve the hydrophobicity of the films (Huan et al., 2015). The hydrophilicity tested was done because the morphologies of silk/PVA based scaffold in this study does not achieved the ideal scaffold where it form a lots of beaded and not uniformity of fibers with small pore size distribution which lead to high surface roughness. Thus water contact angle is used to identify the wettability of silk/PVA based scaffold. The water contact angle of electrospun silk/PVA mats fabricated from using different voltage and flow rate were shown in Figure 4.14 with same concentration of 14% (w/v) for 45 seconds.

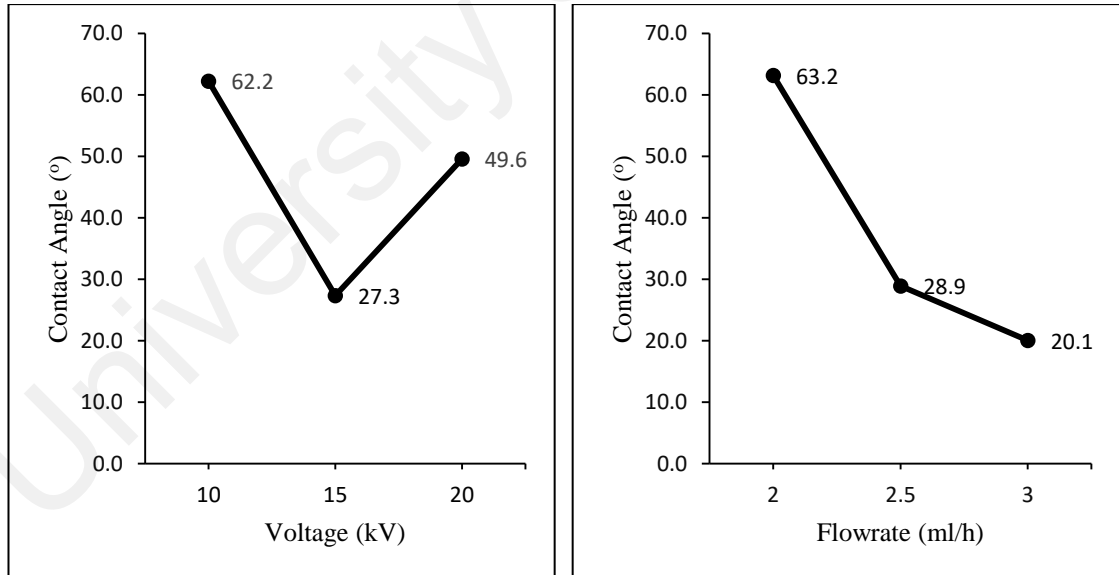


Figure 4.14: Contact angle of electrospun silk/PVA fiber mat with different voltage and flowrate

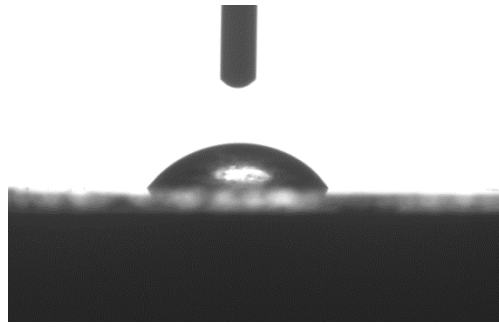


Figure 4.15: Water droplet on electrospun Silk/PVA fibers

In Figure 4.14, it is showed that silk/PVA fiber mat wettability at different applied voltage where the contact angle (CA) value for voltage at 15 kV is 27.3 °, while at 10 kV and 20 kV the measured contact angles are 62.2° and 49.6 ° respectively. The CA value decreased with increased flow rate where the smallest CA value was 20.1° at 3ml/h and highest 63.2 ° at 2 ml/h. The actual performance of a water droplet on the surface of electrospun silk/PVA fiber 14% (w/v), 2.5 ml/h and 20 kV is shown in Figure 4.15. Contact angle that less than 90° indicates high wettability with the fluid spread over large area of the surface. For contact angle that greater than 90 ° means that lower wettability where fluid have minimize contact with surface and formed liquid droplet. Generally, the lower the contact angle, the more hydrophilic the surface of film (Grodzka & Pomianowski, 2006).

Previous studies showed the relationship between hydrophilic surfaces with attachment on the surface. For example, mouse fibroblast generally showed good spreading, proliferation and differentiation when CA were less than 60 °. Not only that, the fibroblast demonstrated accelerated metabolic activity and more fractal morphology on hydrophilic surface. Osteoblast generally favorable to attach and differentiation on hydrophilic surface compare to hydrophobic surface. Adhesion of osteoblast was also reported to decreased with increased of CA of surface from 60 ° to 106 ° (Wei et al., 2007, 2009).

4.4 Identification of chemical compound

The characterization of chemical compound can be determined by FTIR spectra of the Silk/PVA based scaffold. The FTIR becoming important method to study protein secondary structure. The transmission spectra of synthesis proses of silk which are cocoon, degummed silk, regenerated silk fibroin and silk/PVA in the range between 450 to 4000 cm^{-1} . Figure 4.16 shows the comparison spectrum of silk from raw cocoon to silk/PVA solution. There are some similarity of peak in all samples which is hydroxyl group and Amide I. The bands at 3268-3303 cm^{-1} were attributed to the hydroxyl group in silk. The hydroxyl group band become stronger at silk/PVA solution due high intermolecular bonding of O-H. At degummed silk, there is a band at 2978 cm^{-1} attributed to the saturated C-H groups (CH_3). The bands at 1045 to 1065, cm^{-1} were attributed by the C-O stretching mode that represent degummed silk, cocoon, and regenerated silk fibroin respectively. The band at 874 to 879 cm^{-1} were attributed by the C-H bending mode that can be found in regenerated silk and degummed silk. All samples have peaks at 639 to 658 cm^{-1} that were attributed by the NH_2 groups. (Zarei et al., 2013)

Amide I and amide II bands are two major bands of the protein infrared spectrum. The band of amide I (1600 to 1700 cm^{-1}) can be found on all sample that were assigned to the C=O groups and can be directly related to peptide backbone conformation. As can be observed, the position of amide I band shifted to left after regenerated silk blending with PVA which implies that silk structure had interaction with PVA. The band amide II (1515- 1518 cm^{-1}) that result from N-H bending vibration can be found on all sample except Silk/PVA solution. The possibility of amide II absence in silk/PVA solution due to PVA have altered the some functional group of silk. After cocoon were treated with sodium carbonate, there are presence of amide III at degummed silk at 1445 cm^{-1} . This new functional group can be explained where the sericin protein have been removed completely.

These amide I and amide II correspond to the β sheet secondary protein structure of silk protein. Multiple repeats of amino acid sequences for example Gly, Try and As to make up the β sheet. This region indicates the increasing of crystallinity where also can further increasing the strength of the material (H. Zhang et al., 2012). According to Udaseen et al., 2014, the addition of PVA could improve the electrospinning of silk by stabilizing the bond between the silk molecules.

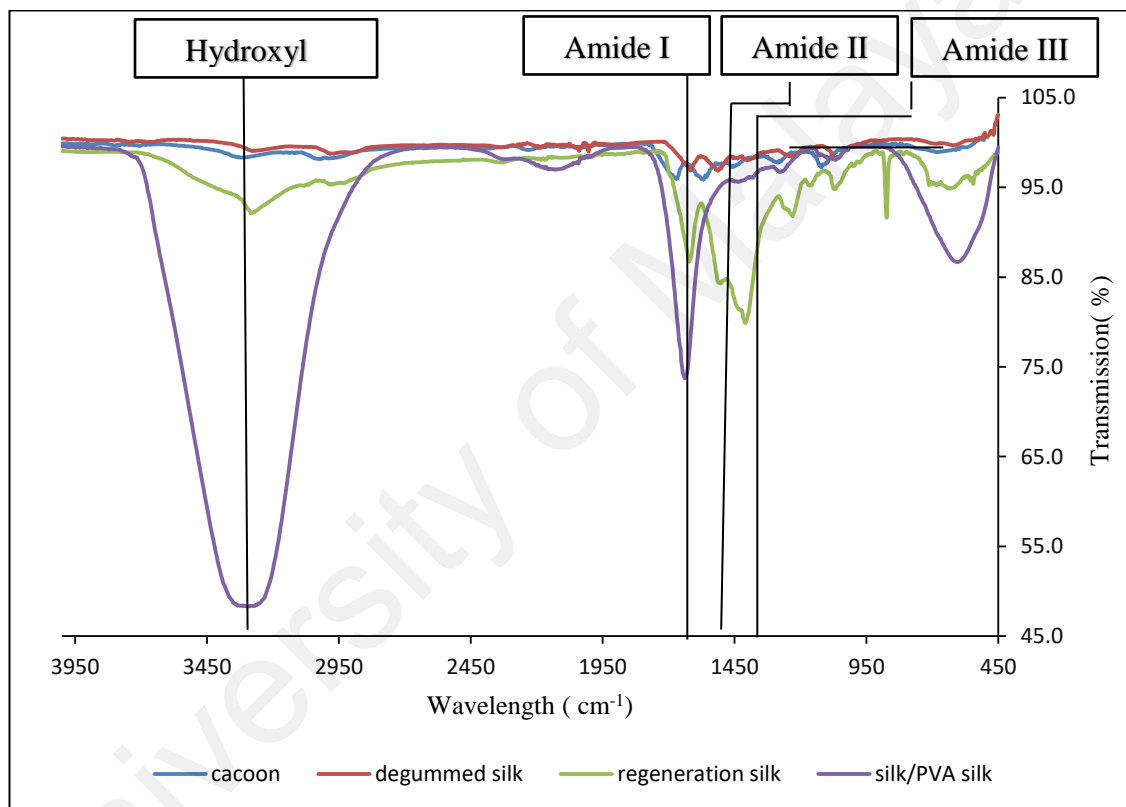


Figure 4.76: The FTIR spectrum of cocoon, degummed silk, regenerated silk and silk/PVA based scaffold

CHAPTER 5: CONCLUSION AND FUTURE STUDIES

In this present study, Silk/PVA films were successfully produced by using dialysis free method where the regenerated silk fibroin was directly mixed with PVA solution. The result presented clearly demonstrate that the parameters such as solution concentration, voltage and flowrate have influences towards fibers morphologies. Various surface morphologies including fiber diameter, beads and pore size have been observed. It was found that the increased of concentration, voltage and flowrate were able to produce more fibers in the film. A thin white film was produced at silk/PVA at 14% (w/v) without addition of chloroform. The fiber diameter of silk film at applied voltage 15kV and flowrate at 3ml/h has the narrowest of average fiber diameter with less number of beaded and smaller in size. The contact angle measures the hydrophilicity of silk film where at 15 kV and 3 ml/h has the lowest value of contact angle which are 27.3 ° and 20.1° respectively. Based on this result, high hydrophilicity and morphologies of electrospun silk/PVA fibers with 14% (w/v) without addition of chloroform, 15 kV with flowrate at 3 ml/h may result in better mechanical stability and better in cell attachment, migration and proliferation that has potential in many biomedical application. The characterization of chemical compound in cocoon, degummed silk, regenerated silk fibroin and silk/PVA solution were determined by FTIR. There are some similarity of peak for all samples which is Hydroxyl group at bands 3268-3303 cm^{-1} and Amide I (1600 to 1700 cm^{-1}). The band amide II (1515- 1518 cm^{-1}) can be found in all samples except for PVA/silk solution. The conformation of β sheet correspond to the band at amide I, amide II and amide III. The amide III was observed in degummed silk, regenerated silk and silk/PVA solution. This shows that sericin protein have been removed completely. The result also indicated that all peaks at silk/PVA solution have become stronger with addition of PVA content through chemical bonding.

Future test that could be carried out is the degradation testing to determine the degradation rate of silk/PVA based scaffold. The degradation rate of a matrix is essential as biomaterial in tissue engineering applications. The silk/PVA film can be immersed in Phosphate Buffer Saline for few days. Besides, the mechanical testing can be employ to determine the mechanical strength of Silk/PVA based scaffold and compare with pure silk fibroin based scaffold and PVA based scaffold. The universal testing machine can be used to carry out the tensile strength of each scaffolds. This analysis would be determine which scaffold has appropriate mechanical strength that suitable as biomaterial. Another recommendation is cytotoxicity test that study interaction and behavior of cells in the silk/PVA based scaffold. The cytotoxicity test can be done by cell culture assay. The cytotoxic test is important to select silk/PVA scaffold as biomaterial in tissue engineering.

REFERENCES

- Addis, K. ., & Raina, S. . (2013). Dissolution Properties of Silk Cocoon Shells and Degummed Fibers from African Wild Silkmths. *Pakistan Journal of Biological Sciences*. doi:10.3923/pjbs.2013.1199.1203
- Agarwal, S., Wendorff, J. H., & Greiner, A. (2008). Use of electrospinning technique for biomedical applications. *Polymer*, 49(26), 5603–5621. doi:10.1016/j.polymer.2008.09.014
- Bowlin, G. L., Sell, S. A., Wolfe, P. S., Garg, K., McCool, J. M., & Rodriguez, I. A. (2010). The Use of Natural Polymers in Tissue Engineering: A Focus on Electrospun Extracellular Matrix Analogues, (2), 522–553. doi:10.3390/polym2040522
- Bressner, J., & Tilburey, G. (2016). Dialysis-Free Process for Aqueous Regenerated Silk Fibroin Solution and Products Thereof. Google Patents. Retrieved from <https://www.google.com/patents/US20160215030>
- Cai, Y., Guo, J., Chen, C., Yao, C., Chung, S., Yao, J., ... Kong, X. (2016). Silk fi broin membrane used for guided bone tissue regeneration. *Materials Science & Engineering C*, 70, 148–154. doi:10.1016/j.msec.2016.08.070
- Caló, E., & Khutoryanskiy, V. V. (2015). Biomedical applications of hydrogels: A review of patents and commercial products. *European Polymer Journal*, 65, 252–267. doi:10.1016/j.eurpolymj.2014.11.024
- Cao, Y., & Wang, B. (2009). Biodegradation of Silk Biomaterials, 1514–1524. doi:10.3390/ijms10041514
- Chang Yang, J., Yang Lee, S., Chien, C. W., Yun, T. H., Da Wu, H., & Yu Ji, D. (2012). High Yield Dialysis-Free Process For Producing Organosoluble Regenerated Silk Fibroin.
- Cheung, H., & Lau, K. (2007). STUDY ON A SILKWORM SILK FIBER / BIODEGRADABLE POLYMER BIOCOMPOSITE.
- D. Ulery, B., S. Nair, L., & T. Laurecin, C. (2012). Biomdical Applications of Biodegradable Polymers, 49(12), 832–864. doi:10.1002/polb.22259.Biomedical
- Daithankar, A. V, Padamwar, M. N., Pisal, S. S., Paradkar, A. R., & Mahadik, K. R. (2005). Moisturizing efficiency of silk protein hydrolysate : Silk fibroin. *India Journal of Biotechnology*, 4(January), 115–121.
- Eichhorn, S. J., & Sampson, W. W. (2010). Relationships between specific surface area and pore size in electrospun polymer fibre networks, (October 2009), 641–649.
- Gimenes, M. L., Silva, V. R., Vieira, M. G. A., Silva, M. G. C., & Scheer, A. P. (2014). High Molecular Sericin from Bombyx mori Cocoons : Extraction and Recovering

by Ultrafiltration. *International Journal of Chemical Engineering and Application*, 5(3), 266–271. doi:10.7763/IJCEA.2014.V5.391

- Goto, Y., Tsukada, M., & Minoura, N. (1990). Molecular cleavage of silk fibroin by an aqueous solution of lithium thiocyanate, 59, 402–209.
- Grodzka, J., & Pomianowski, A. (2006). Wettability versus hydrophilicity, 40, 5–18.
- Gunatillake, P. A., & Adhikari, R. (2003). Biodegradable synthetic polymers for tissue engineering, 5, 1–16.
- He, J., Guo, N., & Cui, S. (2011). Structure and Mechanical Properties of Electrospun Tussah Silk Fibroin Nonofibres: Variation in Processing Parameter. *Iranian Polymer Journal*, 20(9), 713–724.
- Hinderer, S., Lee, S., & Schenke-layland, K. (2016). ECM and ECM-like materials — Biomaterials for applications in regenerative medicine and cancer therapy. *Advanced Drug Delivery Reviews*, 97, 260–269. doi:10.1016/j.addr.2015.11.019
- Huan, S., Liu, G., Han, G., Cheng, W., Fu, Z., Wu, Q., & Wang, Q. (2015). Effect of Experimental Parameters on Morphological, Mechanical and Hydrophobic Properties of Electrospun Polystyrene Fibers, 2718–2734. doi:10.3390/ma8052718
- Huang, X., Bai, S., Lu, Q., Liu, X., Liu, S., & Zhu, H. (2015). Osteoinductive-nanoscaled silk/HA composite scaffolds for bone tissue engineering application. *Journal of Biomedical Materials Research Part B: Applied Biomaterials*, 103(7), 1402–1414. doi:10.1002/jbm.b.33323
- Jacobs, V., Anandjiwala, R. D., & Malik, M. (2010). The Influence of Electrospinning Parameters on the Structural Morphology and Diameter of Electrospun Nanofibers. *Journal of Applied Polymer Science*, (115), 3130–3136.
- Jin, H.-J., Park, J., Valluzzi, R., Cebe, P., & Kaplan, D. L. (2004). Biomaterial films of Bombyx mori silk fibroin with poly(ethylene oxide). *Biomacromolecules*, 5(3), 711–7. doi:10.1021/bm0343287
- Kamalha, E., Zheng, Y. S., Zeng, Y. C., & Mwasiagi, J. I. (2014). Effect of solvent concentration on morphology of electrospun Bombyx mori silk, 39(June), 201–203.
- Karakas, H. (2014). ELECTROSPINNING OF NANOFIBERS AND THEIR APPLICATIONS, 3, 126–131.
- Koh, L., Cheng, Y., Teng, C., Khin, Y., Loh, X., Tee, S., ... Han, M. (2015). Progress in Polymer Science Structures , mechanical properties and applications of silk fibroin materials. *Progress in Polymer Science*, 46, 86–110. doi:10.1016/j.progpolymsci.2015.02.001
- Lee, K., Kim, H., Bang, H., Jung, Y., & Lee, S. (2003). The change of bead morphology formed on electrospun polystyrene fibers. *Polymer*, 44(14), 4029–4034. doi:10.1016/S0032-3861(03)00345-8

- Luo, Z., Zhang, Q., Shi, M., Zhang, Y., Tao, W., & Li, M. (2015). Effect of Pore Size on the Biodegradation Rate of Silk Fibroin Scaffolds, *2015*, 1–8.
- Marelli, B., Brenckle, M. A., Kaplan, D. L., & Omenetto, F. G. (2016). Silk Fibroin as Edible Coating for Perishable Food Preservation. *Nature Publishing Group*, (April), 1–11. doi:10.1038/srep25263
- Meinel, A. J., Kubow, K. E., Klotzsch, E., Garcia-fuentes, M., Smith, L., Vogel, V., ... Meinel, L. (2013). Optimization strategies for electrospun silk fibroin tissue engineering scaffolds, *30*(17), 3058–3067. doi:10.1016/j.biomaterials.2009.01.054.Optimization
- Miyaguchi, Y., & Hu, J. (2005). Physicochemical Properties of Silk Fibroin after Solubilization Using Calcium Chloride with or without Ethanol. *Food Science and Technology Research*, *11*(1), 37–42. doi:10.3136/fstr.11.37
- Navone, S. E., Pascucci, L., Dossena, M., Ferri, A., Invernici, G., Acerbi, F., ... Parati, E. A. (2014). Decellularized silk fibroin scaffold primed with adipose mesenchymal stromal cells improves wound healing in diabetic mice, 1–15.
- Nualkaew, N., Wongsangta, N., & Damrongrungrueng, T. (2012). Effect of fibroin gel from Thai silk cocoon on color extract of *Rosa* spp . flowers. *JAASP*, *1*(2), 116–124.
- Park, J., Yang, C., Jung, I., Lim, H., Lee, J., Jung, U., ... Choi, S. (2015). Regeneration of rabbit calvarial defects using cells-implanted nano-hydroxyapatite coated silk scaffolds, 1–10. doi:10.1186/s40824-015-0027-1
- Pramanik, S., Pinguan-Murphy, B., & Abu Osman, N. A. (2012). Progress of key strategies in development of electrospun scaffolds: bone tissue. *Science and technology of advanced materials*, *13*(4), 043002. doi:10.1088/1468-6996/13/4/043002
- Ri, Y., Woo, H., Min, J., Kim, D., Joo, O., & Hum, C. (2016). Three dimensional electrospun silk fibroin nanofiber for skin tissue engineering. *International Journal of Biological Macromolecules*. doi:10.1016/j.ijbiomac.2016.07.047
- Rnjak-Kovacina, J., & Weiss, A. S. (2011). Increasing the pore size of electrospun scaffolds. *Tissue engineering. Part B, Reviews*, *17*(5), 365–72. doi:10.1089/ten.teb.2011.0235
- Rockwood, D. N., Preda, R. C., Yücel, T., Wang, X., Lovett, M. L., & Kaplan, D. L. (2011). Materials fabrication from *Bombyx mori* silk fibroin, (September). doi:10.1038/nprot.2011.379
- Singh, B. N., Panda, N. N., & Pramanik, K. (2016). A novel electrospinning approach to fabricate high strength aqueous silk fibroin nanofibers. *International Journal of Biological Macromolecules*, *87*, 201–207. doi:10.1016/j.ijbiomac.2016.01.120

- Subramanian, A., Krishnan, U. M., & Sethuraman, S. (2009). Development of biomaterial scaffold for nerve tissue engineering : Biomaterial mediated neural regeneration, *11*, 1–11. doi:10.1186/1423-0127-16-108
- Tang, X.-P., Si, N., Xu, L., & Liu, H.-Y. (2014). Effect of flow rate on diameter of electrospun nanoporous fibers. *Thermal Science*, *18*(5), 1447–1449. doi:10.2298/TSCI1405447T
- Thenmozhi, N., Gomathi, T., & Sudha, P. N. (2013). Preparation and characterization of biocomposites : Chitosan and silk fibroin, *5*(4), 88–97.
- Udaseen, S., Asthana, S., Raveendran, N. T., Kumar, K., Samal, A., Pal, K., ... Ray, S. S. (2014). Optimization of process parameters for nozzle - free electrospinning of poly (vinyl alcohol) and alginate blend nano-fibrous scaffolds, *3*(1), 405–411.
- Vonch, J., Yarin, A., & Megaridis, C. M. (2007). Electrospinning : A study in the formation of nanofibers, *1*.
- Wang, Y., Kim, U.-J., Blasioli, D. J., Kim, H.-J., & Kaplan, D. L. (2005). In vitro cartilage tissue engineering with 3D porous aqueous-derived silk scaffolds and mesenchymal stem cells. *Biomaterials*, *26*(34), 7082–7094. doi:http://dx.doi.org/10.1016/j.biomaterials.2005.05.022
- Wei, J., Igarashi, T., Okumori, N., Igarashi, T., Maetani, T., Liu, B., & Yoshinari, M. (2009). Influence of surface wettability on competitive protein adsorption and initial attachment of osteoblasts. *Biomedical Materials*, *4*(4), 45002. Retrieved from <http://stacks.iop.org/1748-605X/4/i=4/a=045002>
- Wei, J., Yoshinari, M., Takemoto, S., Hattori, M., Kawada, E., Liu, B., & Oda, Y. (2007). Adhesion of mouse fibroblasts on hexamethyldisiloxane surfaces with wide range of wettability. *Journal of Biomedical Materials Research Part B: Applied Biomaterials*, *81B*(1), 66–75. doi:10.1002/jbm.b.30638
- Wei, K., & Kim, I. (2013). Fabrication of Nanofibrous Scaffolds by Electrospinning. *Advance in Nanofibers*.
- Yang, Y., Kwak, H. W., & Lee, K. H. (2013). Effect of Residual Lithium Ions on the Structure and Cytotoxicity of Silk Fibroin Film, *27*(2), 265–270.
- Zarei, M., Gopal, S., C.Lingegowda, D., Kumar, J. K., & Prasad, A. . D. (2013). FTIR SPECTROSCOPIC STUDIES ON CLEOME GYNANDRA – COMPARATIVE ANALYSIS OF FUNCTIONAL GROUP BEFORE, *22*(January 2013), 137–143.
- Zargham, S., Bazgir, S., Tavakoli, A., Rashidi, A. S., & Damerchely, R. (2012). The Effect of Flow Rate on Morphology and Deposition Area of Electrospun Nylon 6 Nanofiber, *7*(4), 42–49.
- Zhang, H., Li, L., Dai, F., Zhang, H., Ni, B., Zhou, W., ... Wu, Y. (2012). Preparation and characterization of silk fibroin as a biomaterial with potential for drug delivery, 1–9.

Zhang, X., R. Reagan, M., & L. Kaplan, D. (2010). Electrospun Silk Biomaterial Scaffolds for regenerative Medicine, *61*(12), 988–1006.
doi:10.1016/j.addr.2009.07.005.Electrospun

Zhang, X., Reagan, R. M., & Kaplan, D. L. (2010). Electrospun Silk Biomaterial Scaffolds for Regenerative Medicine, *61*(12), 988–1006.
doi:10.1016/j.addr.2009.07.005.Electrospun

Zhao, H., Feng, X., Yu, S., Cui, W., & Zou, F. (2005). Mechanical properties of silkworm cocoons, *46*, 9192–9201. doi:10.1016/j.polymer.2005.07.004

University of Malaya

APPENDIX A

Image J software- Fiber diameter

1) Silk/PVA at 14%, 10 kV & 2.5 ml/h

	Area	Mean	StdDev	Min	Max	X	Y	Angle	Length	radius	Diameter
1	2.39	101.35	67.34	0.00	255.00	14.25	91.59	0.37	27.10	0.87	1.75
2	0.05	203.67	23.34	178.00	237.00	50.01	57.34	0.00	0.47	0.12	0.24
3	0.07	208.22	46.29	112.00	255.00	45.49	38.27	60.26	0.68	0.15	0.30
4	0.06	165.25	28.67	117.00	202.00	40.44	52.29	-56.31	0.59	0.14	0.28
5	0.07	173.67	16.89	154.00	207.00	35.22	43.85	-45.00	0.66	0.15	0.30
6	0.06	159.38	15.90	141.00	178.00	30.65	27.83	-71.57	0.63	0.14	0.28
7	0.07	205.78	35.69	142.00	251.00	52.94	52.29	0.00	0.70	0.15	0.30
8	0.05	241.00	9.72	229.00	254.00	60.21	53.47	0.00	0.47	0.12	0.24
9	0.06	201.88	12.97	183.00	223.00	47.01	57.16	9.46	0.60	0.14	0.28
10	0.06	168.50	28.72	121.00	215.00	43.67	57.63	33.69	0.59	0.14	0.28
11	0.06	193.50	34.12	141.00	242.00	45.02	37.28	51.34	0.59	0.14	0.28
12	0.06	198.13	36.94	128.00	243.00	60.04	34.11	51.34	0.59	0.14	0.28
13	0.09	200.46	25.44	160.00	236.00	73.94	28.60	-53.13	0.85	0.16	0.33
14	0.12	178.67	33.35	94.00	229.00	67.49	76.11	21.04	1.26	0.19	0.38
15	0.12	159.00	35.37	106.00	208.00	41.79	76.05	-42.27	1.25	0.19	0.38
16	0.11	210.14	38.36	136.00	252.00	34.52	64.02	38.66	1.17	0.19	0.37
17	0.06	183.00	37.05	129.00	243.00	25.66	44.55	15.95	0.63	0.14	0.28
18	0.05	164.67	43.64	95.00	205.00	58.16	49.01	36.87	0.42	0.12	0.24
19	0.08	212.40	29.78	152.00	250.00	63.20	50.65	0.00	0.82	0.16	0.31
20	0.05	146.29	43.91	80.00	202.00	36.40	49.36	-30.96	0.53	0.13	0.26
21	0.06	181.25	21.46	135.00	204.00	35.58	43.32	-33.69	0.59	0.14	0.28

2) Silk/PVA at 14%, 15 kV & 2.5 ml/h

	Area	Mean	StdDev	Min	Max	X	Y	Angle	Length	radius	diameter
1	2.36	144.02	35.90	0.00	225.00	14.15	90.74	-0.37	26.90	0.87	1.73
2	0.13	140.77	29.27	87.00	178.00	63.76	39.74	-39.81	1.36	0.20	0.41
3	0.05	138.43	12.90	124.00	164.00	72.23	17.90	-18.44	0.55	0.13	0.26
4	0.08	133.55	21.56	93.00	165.00	48.04	26.64	-90.00	0.87	0.16	0.33
5	0.07	127.00	33.76	76.00	164.00	33.89	34.41	-90.00	0.70	0.15	0.30
6	0.08	137.10	30.73	90.00	175.00	16.42	6.46	-26.57	0.78	0.16	0.31
7	0.04	134.20	16.69	113.00	155.00	46.38	23.32	-90.00	0.35	0.11	0.22
8	0.05	135.29	19.75	92.00	148.00	31.94	46.78	-149.04	0.52	0.13	0.26
9	0.04	112.20	12.99	97.00	126.00	26.99	35.31	-75.96	0.37	0.11	0.22
10	0.06	132.25	6.11	121.00	142.00	25.07	27.28	-38.66	0.58	0.14	0.28
11	0.06	183.00	25.95	137.00	215.00	25.07	17.85	-63.44	0.63	0.14	0.28
12	0.06	121.13	18.45	89.00	143.00	29.84	71.64	-38.66	0.58	0.14	0.28
13	0.05	99.86	19.51	66.00	124.00	56.62	65.18	-18.44	0.52	0.13	0.26
14	0.07	100.00	20.81	58.00	116.00	68.27	55.52	-90.00	0.70	0.15	0.30
15	0.06	65.00	19.76	45.00	94.00	69.00	18.66	-8.13	0.59	0.14	0.28
16	0.05	194.17	28.68	149.00	233.00	51.85	29.49	53.13	0.42	0.12	0.24
17	0.03	135.00	1.83	133.00	137.00	51.62	25.94	-90.00	0.23	0.10	0.20
18	0.06	87.25	22.13	65.00	118.00	51.50	23.20	-90.00	0.58	0.14	0.28
19	0.06	131.38	29.36	88.00	169.00	40.90	23.67	-74.06	0.63	0.14	0.28
20	0.02	58.50	27.58	39.00	78.00	28.62	27.69	180.00	0.12	0.07	0.14
21	0.07	62.56	20.90	36.00	93.00	38.57	27.45	180.00	0.70	0.15	0.30

3) Silk/PVA at 14%, 20 kV & 2.5 ml/h

	Area	Mean	StdDev	Min	Max	X	Y	Angle	Length	radius	diameter
1	2.39	182.61	20.95	0.00	185.00	14.25	91.51	0.00	27.10	0.87	1.75
2	0.08	120.18	26.25	67.00	149.00	57.69	41.97	0.00	0.82	0.16	0.31
3	0.10	114.99	26.63	72.00	150.44	45.43	56.28	-61.39	1.05	0.18	0.36
4	0.09	154.94	15.63	130.56	172.18	25.14	55.70	-90.00	0.94	0.17	0.34
5	0.14	162.51	42.73	67.00	213.50	37.22	28.36	-37.57	1.50	0.21	0.42
6	0.12	213.68	15.74	190.65	235.46	64.73	47.60	-33.69	1.27	0.19	0.38
7	0.09	82.42	28.25	39.44	115.95	23.26	37.98	53.13	0.85	0.16	0.33
8	0.12	196.84	38.54	110.67	240.17	24.67	31.53	23.20	1.26	0.19	0.38
9	0.12	216.81	26.61	170.44	247.40	64.26	47.89	-63.44	1.21	0.19	0.38
10	0.12	124.00	35.27	48.33	160.83	52.59	67.08	8.75	1.20	0.19	0.38
11	0.09	178.78	29.34	133.00	212.04	37.22	28.42	-19.98	1.00	0.17	0.34
12	0.10	134.05	14.70	117.89	161.00	20.79	36.75	-90.00	1.06	0.18	0.36
13	0.09	151.90	26.63	114.68	180.16	24.90	49.71	-32.01	0.85	0.16	0.33
14	0.05	144.91	20.11	107.00	158.80	38.74	73.29	0.00	0.47	0.12	0.24
15	0.09	142.98	28.28	85.78	173.98	58.81	68.66	-36.87	0.92	0.16	0.33
16	0.08	245.74	13.35	212.89	254.61	71.06	56.22	45.00	0.83	0.16	0.31
17	0.07	179.48	13.34	160.56	196.00	62.44	25.72	14.04	0.71	0.15	0.30
18	0.09	172.73	10.32	155.78	185.43	48.89	20.27	33.69	0.95	0.17	0.34
19	0.12	118.43	28.30	66.00	149.80	51.16	74.17	42.27	1.31	0.20	0.40
20	0.08	201.07	9.46	185.50	212.67	69.89	70.89	-5.71	0.83	0.16	0.31
21	0.09	115.49	22.52	75.00	137.61	63.73	72.82	-90.00	0.94	0.17	0.34

4) Silk/PVA at 14%, 15 kV & 2 ml/h

	Area	Mean	StdDev	Min	Max	X	Y	Angle	Length	radius	diameter
1	2.46	168.11	5.71	143.00	225.00	14.82	93.95	0.00	27.10	0.88	1.77
2	0.09	190.73	54.78	65.00	234.00	40.65	49.41	36.87	0.90	0.17	0.34
3	0.04	174.40	33.27	136.00	224.00	75.79	17.34	-63.44	0.40	0.11	0.23
4	0.07	193.78	24.03	157.00	227.00	82.02	30.89	0.00	0.72	0.15	0.30
5	0.07	237.38	14.49	210.00	254.00	63.60	66.76	-56.31	0.65	0.14	0.29
6	0.04	155.80	30.93	125.00	193.00	45.08	72.99	-116.57	0.40	0.11	0.23
7	0.11	103.31	40.56	46.00	174.00	20.69	44.63	-80.54	1.10	0.18	0.37
8	0.07	192.25	14.73	166.00	208.00	24.21	32.07	-123.69	0.65	0.14	0.29
9	0.06	178.29	10.74	164.00	194.00	31.80	28.55	45.00	0.51	0.13	0.27
10	0.06	119.43	23.09	79.00	141.00	46.88	69.59	-63.44	0.54	0.13	0.27
11	0.07	154.89	21.90	114.00	178.00	46.94	50.98	-56.31	0.70	0.15	0.30
12	0.06	116.14	21.15	79.00	137.00	46.04	47.55	-63.44	0.54	0.13	0.27
13	0.07	237.00	24.68	198.00	255.00	37.37	32.79	-38.66	0.60	0.14	0.29
14	0.07	116.00	32.21	71.00	159.00	41.10	77.30	-90.00	0.72	0.15	0.30
15	0.07	81.00	19.63	49.00	109.00	47.06	69.65	-81.87	0.61	0.14	0.29
16	0.05	246.50	13.11	222.00	255.00	53.57	67.54	-101.31	0.50	0.12	0.25
17	0.03	215.75	13.87	202.00	235.00	72.18	75.73	0.00	0.24	0.10	0.20
18	0.03	197.75	12.95	189.00	217.00	63.69	70.19	-71.57	0.27	0.10	0.20
19	0.05	200.33	11.45	183.00	216.00	62.78	64.95	11.31	0.50	0.12	0.25
20	0.05	158.17	22.66	129.00	192.00	74.41	44.17	-36.87	0.43	0.12	0.25
21	0.06	89.71	48.85	17.00	140.00	76.21	40.74	-45.00	0.51	0.13	0.27

5) Silk/PVA at 14%, 15 kV & 3 ml/h

	Area	Mean	StdDev	Min	Max	X	Y	Angle	Length	radius	diameter
1	2.39	1.21	14.96	0.00	185.00	14.69	92.20	0.00	26.90	0.87	1.74
2	0.09	137.10	61.93	48.98	209.98	54.01	52.36	-53.13	0.92	0.17	0.33
3	0.06	182.88	9.54	176.00	203.11	68.58	38.43	-63.44	0.53	0.13	0.26
4	0.09	116.84	23.63	74.33	146.33	69.76	30.29	11.31	0.97	0.17	0.35
5	0.09	227.73	15.89	189.00	245.48	51.77	21.97	23.96	0.90	0.17	0.33
6	0.14	199.78	45.92	77.33	246.90	40.73	26.16	-17.35	1.49	0.21	0.42
7	0.11	172.76	36.98	120.11	228.09	33.30	74.30	-90.00	1.18	0.19	0.37
8	0.08	93.11	47.12	9.33	144.55	31.18	77.43	-130.60	0.76	0.16	0.32
9	0.13	162.99	20.64	118.12	189.26	27.46	63.98	-104.93	1.35	0.20	0.40
10	0.11	113.10	36.99	35.67	163.00	30.29	54.71	-120.96	1.11	0.19	0.37
11	0.11	156.13	29.67	83.00	193.65	38.49	46.69	-126.03	1.18	0.19	0.37
12	0.09	124.64	30.79	76.00	172.90	38.91	21.27	-55.01	1.02	0.17	0.35
13	0.09	148.40	19.30	105.00	172.33	38.91	40.14	-23.96	0.90	0.17	0.33
14	0.09	167.18	30.28	111.56	203.55	38.96	46.69	-135.00	1.00	0.17	0.35
15	0.11	117.00	41.07	41.44	168.53	30.35	54.89	-112.62	1.16	0.19	0.37
16	0.11	148.94	31.17	90.67	186.46	26.10	71.11	-90.00	1.18	0.19	0.37
17	0.11	218.32	35.47	122.11	250.26	58.84	78.31	-122.47	1.11	0.19	0.37
18	0.13	197.24	28.20	132.56	241.95	68.99	77.31	-36.87	1.35	0.20	0.40
19	0.07	114.99	26.26	63.56	140.33	71.88	19.67	-90.00	0.71	0.15	0.30
20	0.12	174.50	31.07	136.00	230.86	53.00	18.20	-39.29	1.25	0.19	0.39
21	0.11	171.27	16.13	142.59	202.64	33.65	18.49	-38.66	1.18	0.19	0.37

APPENDIX B

Image J software- Pore Size

1) Silk/PVA at 14%, 10 kV & 2.5 ml/h

Slice	Count	Total Area	Average Size	%Area	Mean
pc,10V,2.5 ml/h	6262	6832.541	1.091	79.22	254.75 3

2) Silk/PVA at 14%, 15 kV & 2.5 ml/h

Slice	Count	Total Area	Average Size	%Area	Mean
pc,15V,2.5 ml/h	3752	5175.336	1.379	60.901	254.41

3) Silk/PVA at 14%, 20 kV & 2.5 ml/h

Slice	Count	Total Area	Average Size	%Area	Mean
pc,20V,2.5 ml/h	12829	4841.221	0.377	54.681	254.378

4) Silk/PVA at 14%, 15 kV & 2 ml/h

Slice	Count	Total Area	Average Size	%Area	Mean
pc,15V,20001.tiff	1412	7732.807	0.547	85.057	254.6

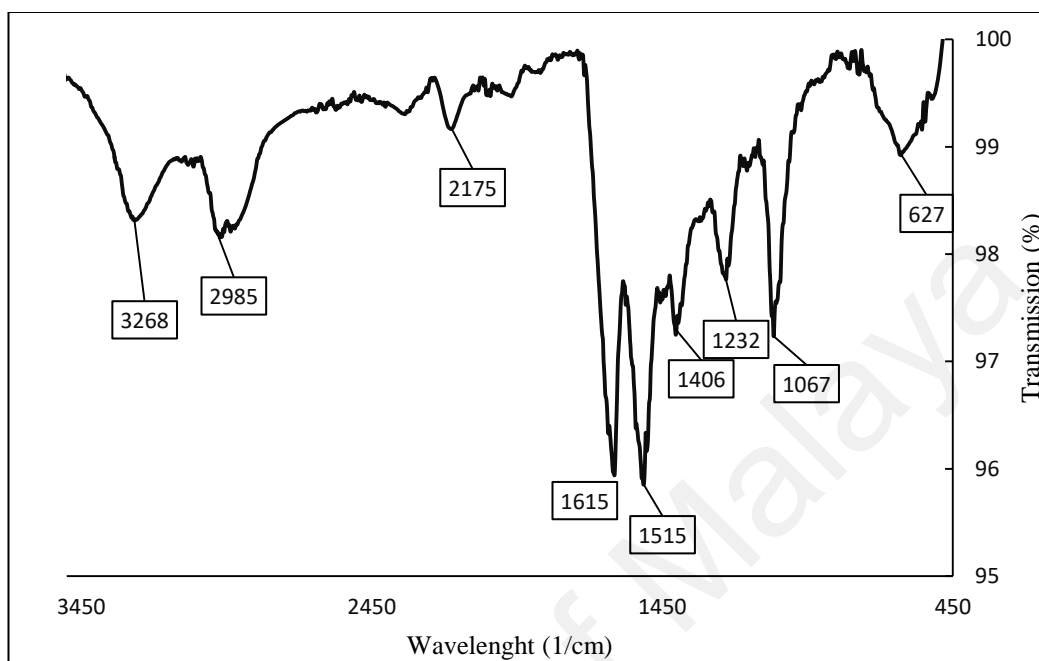
5) Silk/PVA at 14%, 15 kV & 3 ml/h

Slice	Count	Total Area	Average Size	%Area	Mean
pc,20V,2.50004.tiff	7884	5459.195	0.692	64.241	254.242

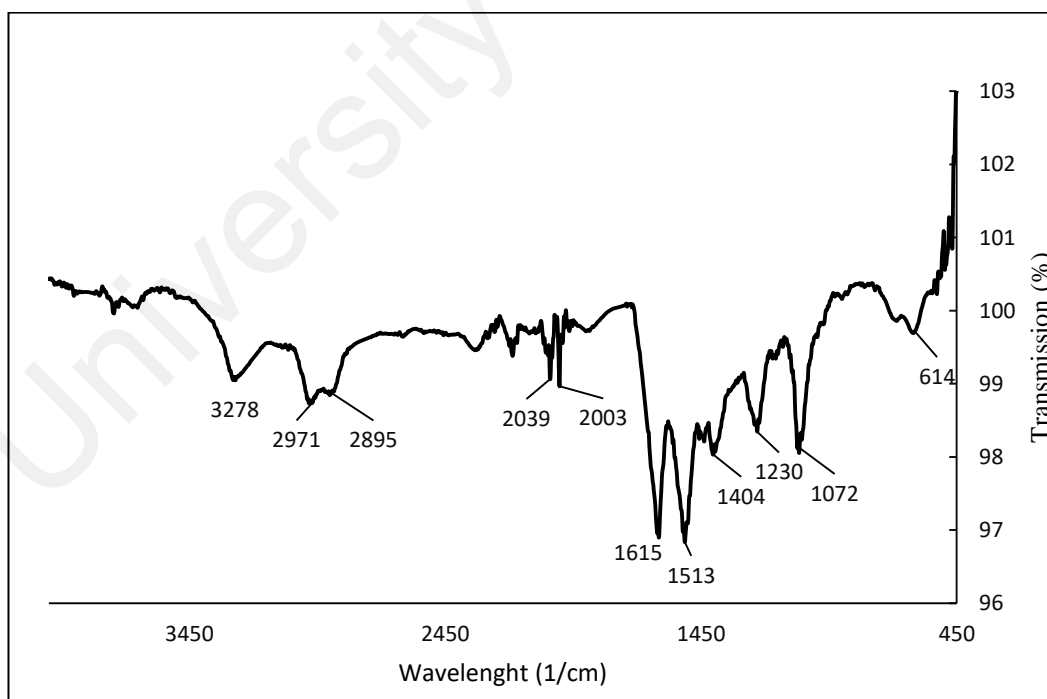
APPENDIX C

FTIR Spectra

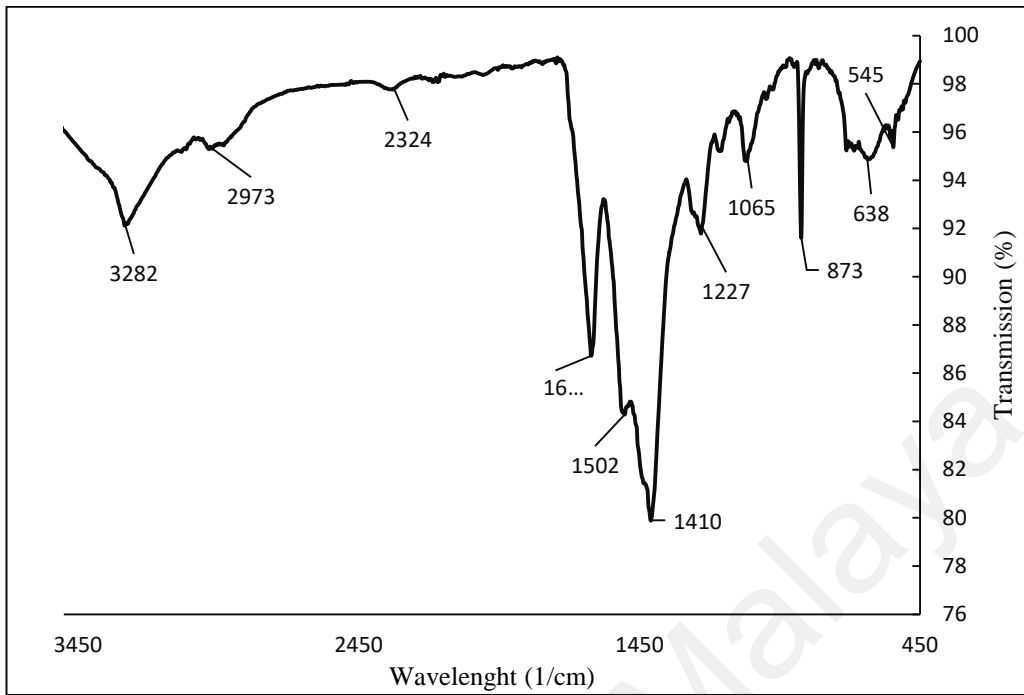
1) Cocoon



2) Degummed Silk



3) Regenerated Silk Fibroin



4) Silk/PVA solution

